

The application of low temperature  
heat engines using shape memory alloys to waste heat  
utilization in electric generating power plants

by

Francis John Wyant

A Thesis Submitted to the  
Graduate Faculty in Partial Fulfillment of the  
Requirements for the Degree of  
MASTER OF SCIENCE

Major: Nuclear Engineering

---

Signatures have been redacted for privacy

Iowa State University  
Ames, Iowa

1980

## TABLE OF CONTENTS

	Page
ABSTRACT	iv
I. INTRODUCTION	1
II. LITERATURE REVIEW	3
III. NITINOL	6
A. Physical Properties	6
B. Inducing the Shape Memory Effect in Nitinol	7
C. Current Non-energy Related Applications of Nitinol	9
1. Fasteners and couplings	9
2. Thermoactuated control devices	9
3. Orthodontic and orthopedic devices	10
4. Blood clot filters	11
IV. LOW TEMPERATURE HEAT ENGINE APPLICATIONS OF NITINOL	12
A. Low Temperature Heat Energy	12
B. Low Temperature Heat Engines Using Nitinol	13
V. NEW LOW TEMPERATURE HEAT ENGINE DESIGN	20
A. Basic Design Characteristics and Principles of Operation	20
B. Construction Details	22
C. Analytical Determination of Work Output	28
D. Estimated Performance	32
1. Pertinent design equations	33
2. Determination of component dimensions	38
3. Calculation of expected work, power, and efficiency	40
VI. APPLICATION TO WASTE HEAT UTILIZATION IN ELECTRIC GENERATING POWER PLANTS	45

	Page
VII. CONCLUSION	47
VIII. REFERENCES	48
IX. ACKNOWLEDGMENTS	51
X. APPENDIX A: CALCULATION OF WORK DONE BY TUBE	52
XI. APPENDIX B: CALCULATION OF PROTOTYPE COMPONENT DIMENSIONS	57
XII. APPENDIX C: HEAT TRANSFER CALCULATIONS FOR PROTOTYPE NITINOL TUBE	65

## ABSTRACT

The application of the shape memory properties of an alloy of nickel and titanium (called Nitinol) to the conversion of low temperature heat into useful mechanical work has been studied. Sources of low temperature heat have been identified. They include the bottoming cycles of commercial power plants, unfocused solar energy, ocean thermal gradients, and spent nuclear fuel elements stored at nuclear power plants. Designs of patented low temperature heat engines using shape memory materials have been studied and their principles of operation determined.

A new low temperature heat engine design is presented along with calculations of the expected work and power output, and conversion efficiency of a design prototype which uses one kilogram of Nitinol. The new design embodies forty-eight Nitinol tubes attached to a central crank which rotates due to the forces applied to it as the tubes undergo temperature induced transformation elongations and contractions. The work output is calculated to be 657.6 ft-lbf with a corresponding power output of 0.44 kilowatts. The total heat input to the engine is 53.8 Btu, resulting in an efficiency of 1.6%. The corresponding Carnot efficiency of 13.9% is based on a hot fluid temperature of 115<sup>o</sup>F and a 35<sup>o</sup>F cold fluid temperature.

A cost of \$2.5 million would be required to purchase the amount of Nitinol necessary in order to scale the design up to a size such that a nuclear power plant could make use of the resulting mechanical work

converted from the heat rejected into the plant's condenser cooling system. However, due to the expected low operating and maintenance costs of the engine the utility can expect a profit of \$6.2 million by selling the useful work output as electricity.

## I. INTRODUCTION

In the years immediately prior to 1973, Americans, who accounted for only six percent of the world's population, were consuming about 30 percent of the world's energy production (1). An oil embargo by the Arab countries against the United States in 1973 caused widespread panic at gas pumps, school shutdowns in the Midwest on cold winter days, and a presidential plea to the nation for conservation of energy resources. Part of the response to the country's awareness of America's dependence on foreign oil supplies was an expanded search for alternative means of energy production which could be had at low cost and high efficiency. This search included renewed interest in solar conversion systems, wind and ocean wave energy utilization, and thermonuclear fusion.

Another, and until recently untapped, source of energy is that available in the heat rejected from electricity generating power plants. These plants dump about two-thirds of the heat generated in their boilers into the condenser cooling water system. This heated water can reach temperatures as high as 115<sup>o</sup>F (2). A means of converting the low temperature heat from these sources into useful mechanical energy exists in heat engine design concepts which use a new breed of metals, the so-called "shape memory" alloys, as the primary driving elements.

Shape memory alloys exhibit the ability to return to a particular shape configuration with considerable force upon slight heating after they have been deformed out of that shape (3). A device which

converts the heat energy contained in hot water into rotary motion was designed and built by Ridgway Banks of Lawrence Berkeley Laboratory in 1973 (4,5,6). Banks' offset crank engine uses twenty U-shaped wires made of Nitinol (nickel-titanium alloy). These wires have "remembered" straight configurations. This shape memory engine has operated for more than  $10^8$  revolutions at speeds between 60 and 80 rpm, with a measured power output of about 0.2 watts (5,7).

This paper contains the design of a new low temperature heat engine which, although similar to the Banks' design, employs the advantages of straight tubes of Nitinol rather than bent wires. Consideration is given to the cost of scaling up the proposed design to a size whereby one or more of these devices may be used to convert a portion of the heat rejected by a nuclear power plant into useful mechanical work. The proposed design will combine a new heat engine technology with the recently defined national goal of energy conservation.

## II. LITERATURE REVIEW

A literature review was made into the areas of the shape memory phenomenon of certain alloys, the history, properties, and current applications of Nitinol. Also surveyed was literature pertaining to sources of low temperature heat, and low temperature heat engine designs which use Nitinol as the active drive element.

As described by Wechsler and Roberts (8), the shape memory behavior exhibited by all shape memory alloys is attributed to the phenomenon known as martensitic phase transformation. All metals are characterized by a regular periodic arrangement of their atoms on a crystal lattice. In many cases, this arrangement changes from one form to another at a given temperature (e.g., pure iron changes from a Body Centered Cubic (BCC) crystal structure to a Face Centered Cubic (FCC) structure upon heating at  $910^{\circ}\text{C}$ ). Sometimes, however, this transformation in structure occurs rapidly by a coordinated shearing motion of atoms. For some martensitic phase transformations, a cyclic change in shape occurs as the metal is cycled from the low-temperature structure to the high-temperature structure and back again. Since the metal "remembers" the shape it had in one or both of these phases, this behavior is known as "shape memory."

The shape memory effect belongs to a more general class of temperature induced phenomena, exhibited by many materials, known as the Joule effect. The Joule effect was first noted by the British physicist



James Prescott Joule in the 19th century. He observed that if stretched rubber is warmed it tends to contract (9).

A. B. Greninger and V. G. Mooradian showed in 1938 that a change in temperature would cause the martensite phase in brass to form or disappear, depending upon whether the metal's temperature was above or below a critical value (10). Remarkably large forces were shown to be developed in Au-Cd alloys by the temperature induced phase transformations by T. A. Read in the 1950s. At about the same time, other research of shape memory behavior was being conducted on such alloys as Fe-Pt, Cu-Al, In-Tl, In-Cd, Fe-Ni, Ag-Zn, and Ni-Al (10,11).

It wasn't until 1962, however, during the course of a search for a tough, non-magnetic, non-corrosive metal for use in underwater tools and equipment, that William J. Buehler and his associates at the U.S. Naval Ordnance Laboratory discovered the Joule effect in an alloy of nickel and titanium. This alloy was found to exhibit the shape memory effect more strongly than any previously investigated material. The alloy was dubbed "Nitinol" for Nickel Titanium Naval Ordnance Laboratory (10,12).

The strong temperature dependent nature of several of Nitinol's physical properties is documented by Jackson et al. (3), Cross et al. (13), and Mohamed (14). Some of the temperature dependent properties discussed are the temperature at which Nitinol transforms while under various loads, the elastic modulus, and the yield stress.

Schetky (10) indicates that some current uses for Nitinol include "weldless" hydraulic-tube couplings for jet fighters and greenhouse window openers. Additional applications for Nitinol are noted by Wayman (11) and Curry (15) such as hot-water valve actuators, clutches for automobile radiator fans, orthodontic dental arch wires, blood clot filters, and orthopedic devices.

Future applications of Nitinol include heat engines for converting low temperature heat to mechanical energy. Ginell et al. (16) list a number of potential sources from which low temperature heat energy may be extracted. These sources include power plants, ocean and freshwater thermal gradients, geothermal heat, and industrial waste heat. An estimate given of the power available from these sources is  $2.1 \times 10^{10}$  Mw.

Several patents (4,17,18,19,20,21) have been issued on low temperature heat engine designs which use Nitinol for converting low temperature heat into useful mechanical work.

### III. NITINOL

A presentation is made of the physical properties of Nitinol including those particularly dependent upon temperature. Also, a step-by-step procedure for inducing the shape memory effect in Nitinol is given. Lastly, some of the non-energy related uses of Nitinol are discussed.

#### A. Physical Properties

Technically, 55-Nitinol is the nickel-titanium alloy containing 53 to 57 percent of nickel by weight, with the balance being titanium (4). By changing the relative amounts of nickel and titanium in a specimen, the temperature at which the alloy transforms will change. The transformation temperature of Nitinol having 55 weight percent nickel in titanium is  $165^{\circ}\text{C}$  while the transformation of Nitinol with 57 weight percent nickel is at  $-26^{\circ}\text{C}$  (3).

Table 1 lists some of Nitinol's other physical properties. The most notable omissions from table 1 are the values of Nitinol's elastic modulus and yield stress. The absence of specific values is due to the fact that these properties are both temperature dependent and depend upon the direction of the temperature change. Figure 1 shows this temperature dependent nature of Nitinol. Note that the upper portion of the figure (A) is for cooling while the lower curves (B) show the behavior upon heating. The temperatures indicated as  $M_s$ ,  $M_f$ ,  $M_d$ , and  $A_s$  are the temperatures at which the Nitinol begins transformation

to the low temperature phase upon cooling ( $M_s$ ), that at which the Nitinol is completely transformed ( $M_f$ ), the largest value that  $M_s$  may be when external stress is applied ( $M_d$ ), and the temperature at which the Nitinol begins the reverse transformation upon heating ( $A_s$ ).

Table 1. Certain physical properties of nominal 55-Nitinol (13)

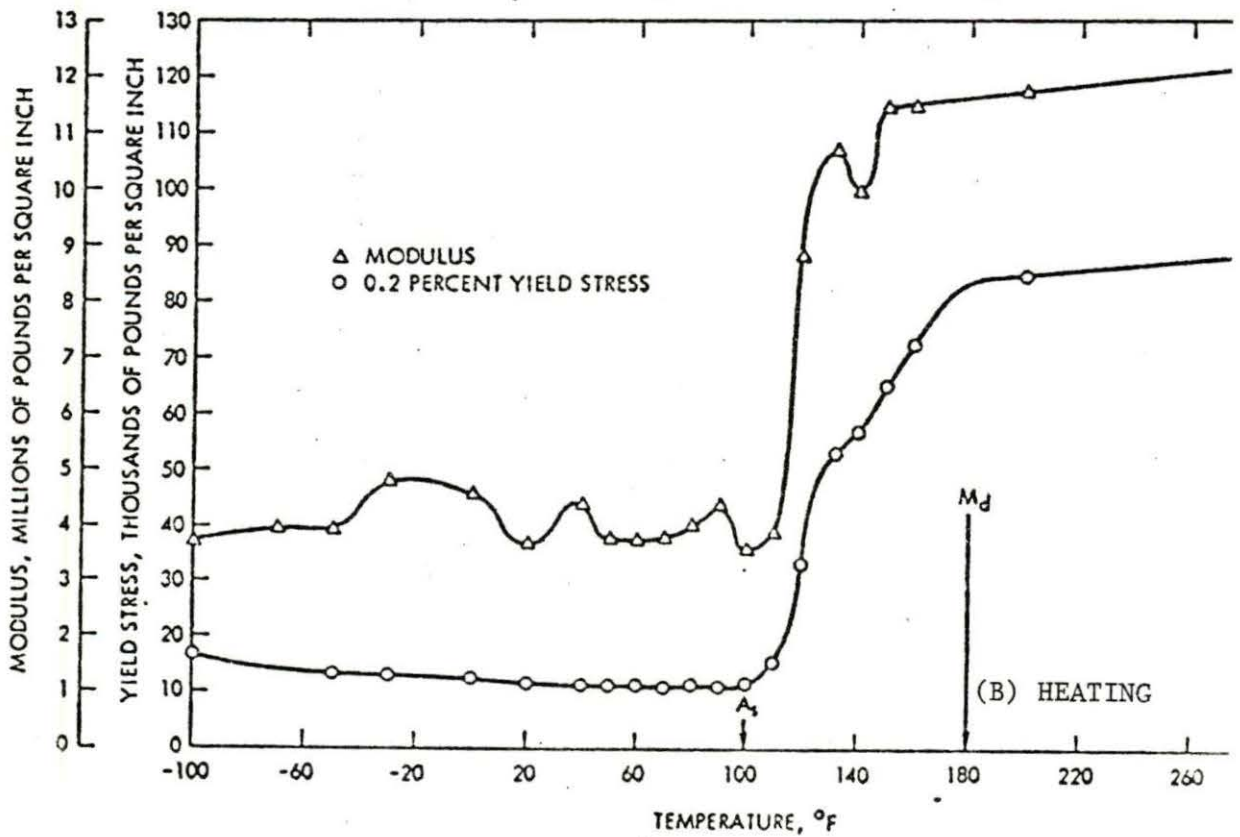
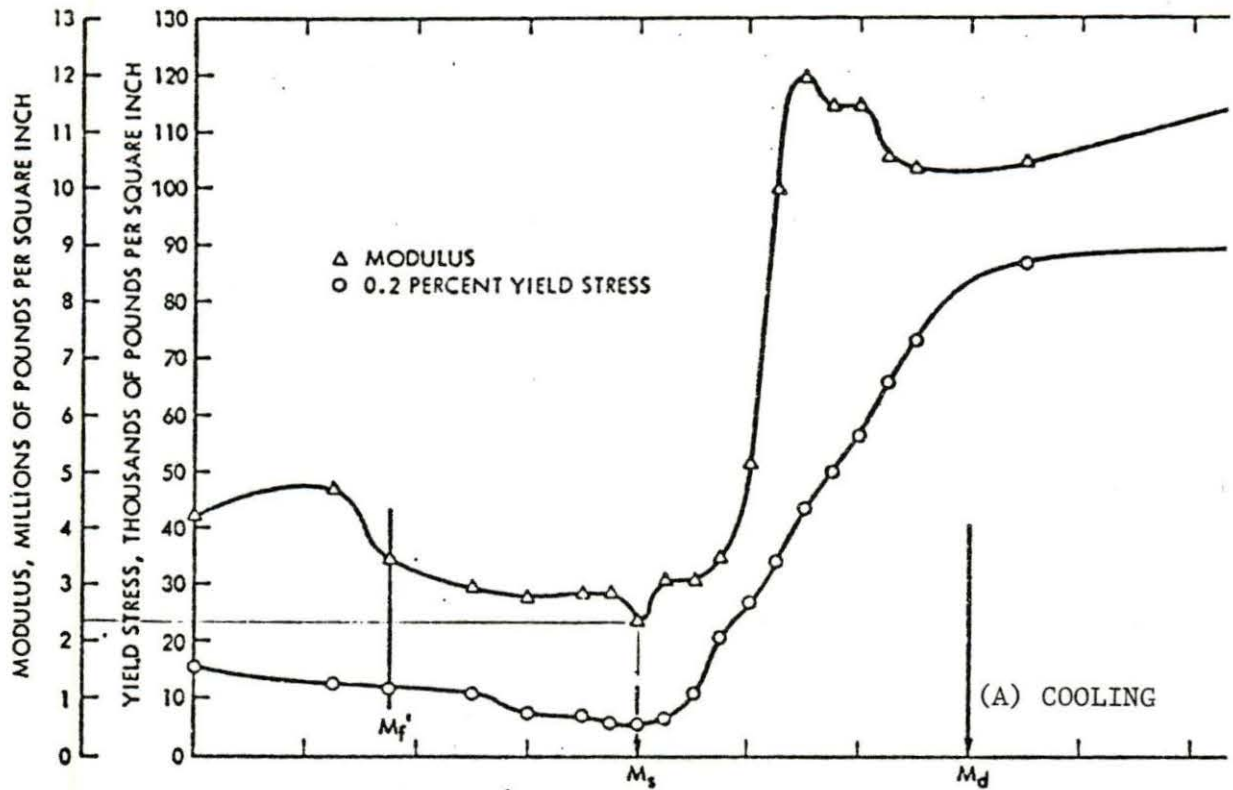
Symbol	Property	Value	Units
$\rho_N$	Density	0.234	lb/in <sup>3</sup>
$T_{mp}$	Melting point	2390	°F
$\bar{r}$	Electrical resistivity		
	at 68°F	80	μohm-cm
	at 1652°F	132	μohm-cm
$\alpha$	Mean coefficient of thermal expansion	5.7	per °F x 10 <sup>-6</sup>
$\nu_N$	Poisson's ratio	0.33	(dimensionless)

#### B. Inducing the Shape Memory Effect in Nitinol

In spite of the fact that Nitinol is called a shape memory alloy, a particular conditioning process is required to produce the shape memory effect in this alloy. The general procedure for Nitinol is listed below (3).

1. Obtain Nitinol in a suitable geometry (e.g., wire, rod, sheet, tube, etc.)
2. Deform the piece into the desired "memory configuration"

Figure 1. Yield stress and elastic modulus of 55-Nitinol as functions of temperature (13)



3. Clamp and constrain the piece in its memory configuration
4. Give a memory heat treatment ( $T=900^{\circ}\text{F}$ ) for 5 to 10 minutes
5. Cool the piece below the transition temperature
6. Strain the piece to some intermediate shape
7. Heat the piece above the transition temperature ( $T \leq 275^{\circ}\text{F}$ )
8. Metal returns to the original high temperature shape

Note that in a cyclic process only steps 5 through 8 need to be repeated in each cycle. Additionally, some shape-memory alloys can be made to develop two-way memory so that in a work cycle step 6 will be changed to read

6. Piece returns to the low temperature shape.

#### C. Current Non-energy Related Applications of Nitinol

The shape memory properties of Nitinol have been applied in a variety of ways by many professions and industries. Among the present uses for Nitinol are (10,11,15):

##### 1. Fasteners and couplings

Nitinol is presently used to join sections of hydraulic line in certain aircraft thus eliminating the deleterious heat effects on the tube material which occur when welding is used to make the connection.

##### 2. Thermoactuated control devices

Nitinol elements have been used in automobile fan clutches by the Delta Memory Metal Company of Suffolk, England. The fan clutch

reduces the load on the engine by engaging the fan only when the radiator water temperature reaches a certain value.

Nitinol springs have also been used to control the extent to which greenhouse windows are open by sensing the inside temperature. Thermostat control devices and hot-water valve actuators are examples of other uses for Nitinol springs.

### 3. Orthodontic and orthopedic devices

Nitinol wire is used in some dental arch braces; when below the transformation temperature the wire is very pliable and thus easily fitted in the patient's mouth. As the wire warms up to body temperature (which is above the transformation temperature), the memory configuration of the brace is such that it applies constant pressure at the appropriate points.

Nitinol bone plates have been suggested for use in compression fixation of bone fractures. Once installed, the bone plate would heat up and as transformation occurred, it would cause the ends of the broken bone to be fitted securely together. Since Ni-Ti is a very inert alloy, the risk of tissue or organ contamination would be minimal and the surgical procedure for installing the device would be simple.

Another suggestion for use of Nitinol in orthopedics is as a Harrington rod used to straighten abnormally bent spines.



#### 4. Blood clot filters

A thin strand of relatively straight Nitinol wire is introduced into a blood vessel where it wads up after transformation and forms a small filter. This filter traps and removes small "wandering" blood clots from the cardio-vascular system thus preventing the potential damage these clots could cause if they were to lodge in the heart, lungs, or extremities.

#### IV. LOW TEMPERATURE HEAT ENGINE APPLICATIONS OF NITINOL

A new and promising area for the application of Nitinol's shape memory properties is in the field of low temperature waste heat utilization. This chapter presents a general discussion of the applicability of using Nitinol in the conversion of low temperature waste heat to useful work, possible sources of this type of heat energy and the work cycle of a Nitinol element with some examples of current low temperature, shape memory heat engine designs.

##### A. Low Temperature Heat Energy

The basic purpose of a heat engine is to convert heat energy available at some temperature into mechanical energy. Most heat engines in use today convert heat stored in some medium at high temperature and pressure and produced by the combustion of fossil fuels or from the atomic interactions in a nuclear reactor. Efficiencies of such systems typically range from 30 to 40 percent (16). Hence, about two-thirds of the heat is rejected to a low temperature and pressure heat sink. A heat engine that has Nitinol as the active element can be used to convert some of this low temperature heat into mechanical energy, thus improving the overall power plant efficiency. In the same way, such a device could convert to useful work some of the heat rejected by commercial manufacturing and processing plants.

Generally, these low-grade heat sources are available at temperatures around  $100^{\circ}\text{C}$  (2). According to Ginell et al. (16) the estimated thermal heat rejection rate for fossil and nuclear power plants operating in the United States is of the order of  $2 \times 10^5$  Mw, based on rejected hot water temperatures of between  $104^{\circ}\text{F}$  and  $194^{\circ}\text{F}$ , and differential temperatures in the range of  $27^{\circ}\text{F}$  to  $117^{\circ}\text{F}$ . Using an estimated Nitinol engine conversion efficiency of ten percent this amount of rejected heat is equivalent to about  $2 \times 10^4$  Mw, corresponding to an estimated savings of about a half-billion barrels of oil per year. This savings is about 25 percent of the oil imported into the United States during the past year (October 1979 through September 1980) (22).

In addition to the low temperature heat energy sources available from industrial and power plant bottoming cycles, other replenishable or previously untapped low temperature heat sources may also be used to power a heat engine featuring Nitinol elements. Some of these low temperature sources include unfocused solar energy, ocean thermoclines, geothermal water, and decay heat generated by spent fuel elements stored onsite at nuclear power plants.

#### B. Low Temperature Heat Engines Using Nitinol

The basic work cycle of a Nitinol element is illustrated in figure 2. As seen in figure 2(a) the Nitinol bar is in the low temperature phase and under no load; in figure 2(b) work ( $W_1 = P_1 Z$ ) has been done on the bar causing it to deform; figure 2(c) the

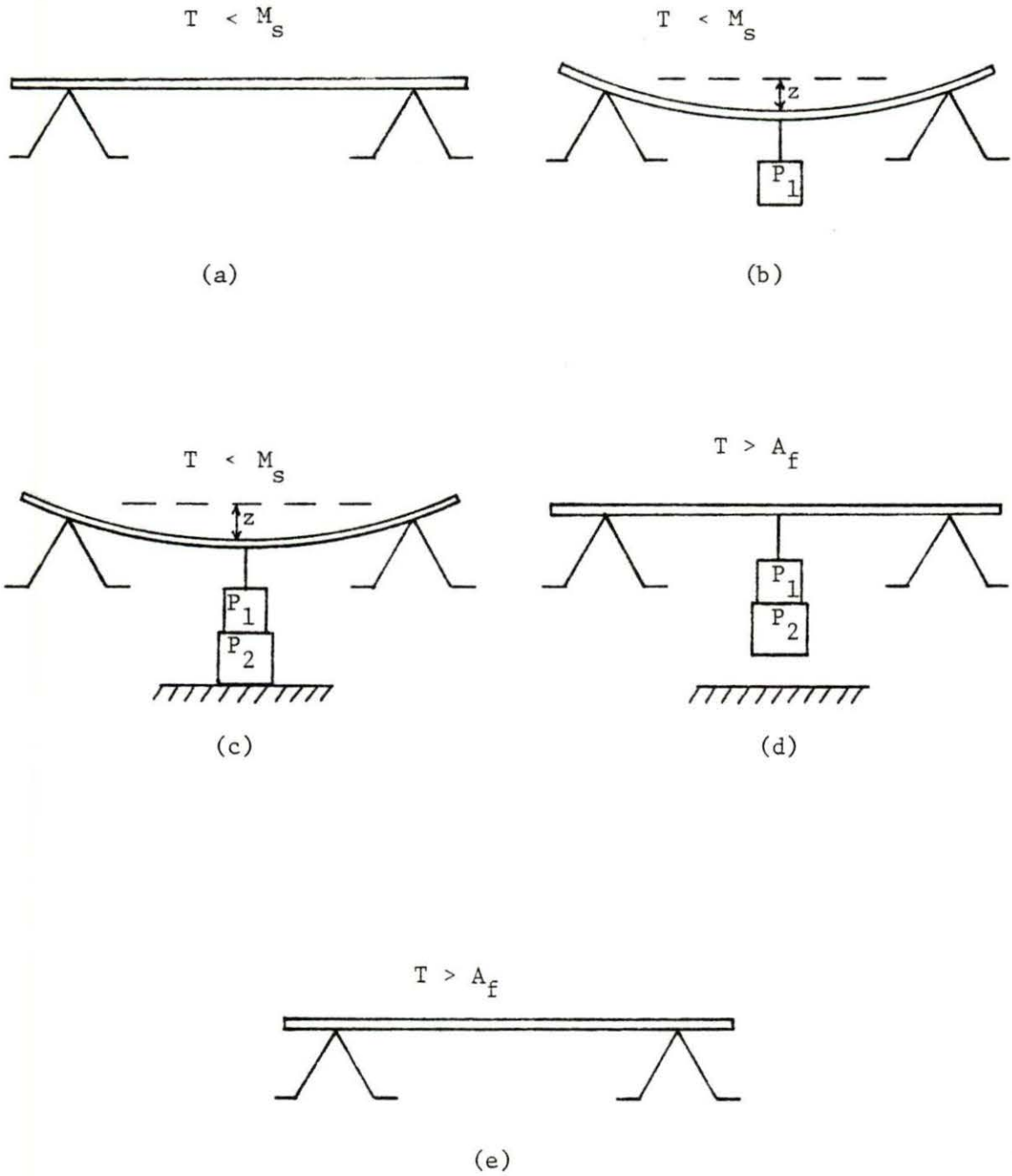


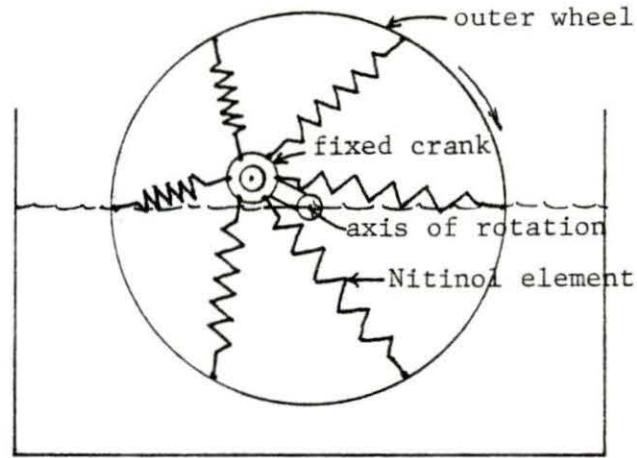
Figure 2. Work cycle of a Nitinol bar (23)

deformation is kept constant as additional load ( $P_2$ ) is connected to the first weight; figure 2(d), the bar is heated and transforms to the high temperature phase, as it transforms it returns to its straight memory configuration and in the process does work ( $W_2 = (P_1 + P_2)Z$ ); figure 2(e), the load is removed and the bar is cooled below the transformation temperature as in figure 2(a). The net work done by the bar during the cycle is

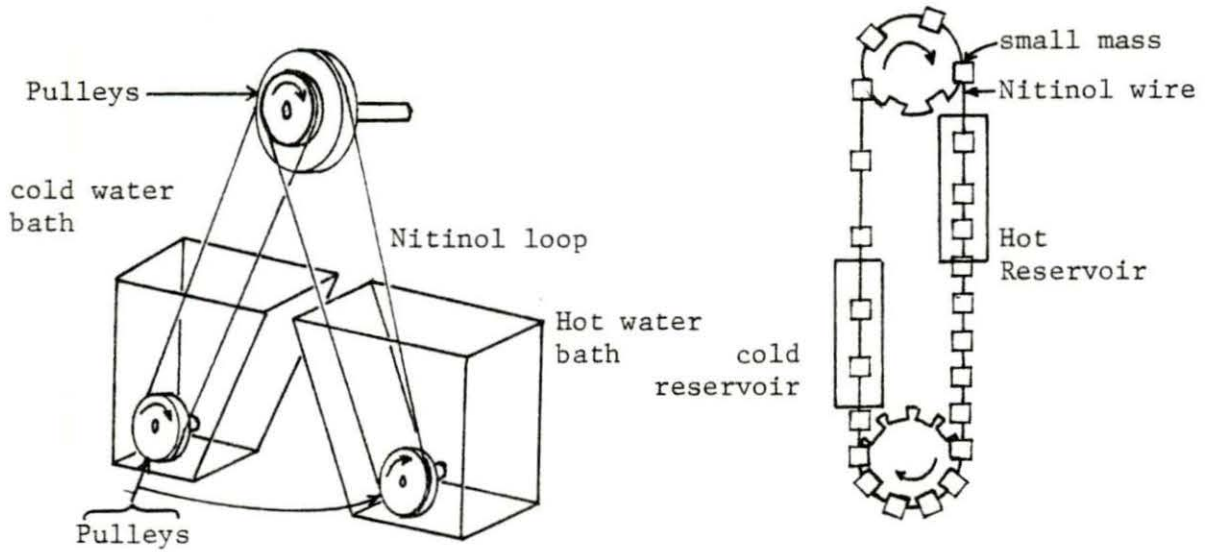
$$W_{\text{net}} = W_2 - W_1 = P_2 Z$$

There are several patented designs which incorporate the Nitinol work cycle. Ginell et al. (7) classify these designs into three types: (1) Offset crank engines, (2) Turbine engines, and (3) Field engines. Figure 3 illustrates examples of these engine types.

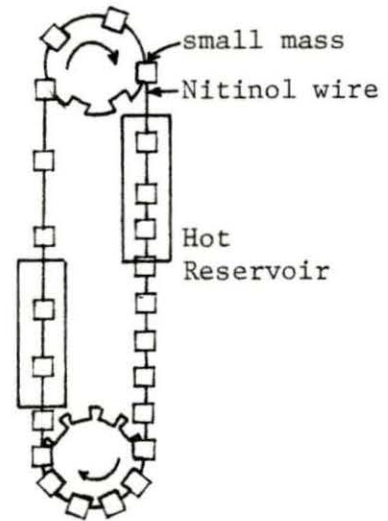
The principle of the offset crank engine is that a number of Nitinol elements in the shape of springs, loops, or twisted plates are fixed to a crank (offset from the center of the device) at one end and to an outer wheel (or other rigid member) at the other end. The Nitinol transforms as the temperature is changed and the resulting force is applied to the non-fixed component (either the crank or outer wheel) to which they are attached. That component of the force which is tangent to the rotating member's direction of motion allows the wheel (or crank) to continue to rotate. As the wheel rotates it carries the Nitinol elements from the source of heat to the heat sink and in this way helps to continue the cycle.



(a)



(b)



(c)

Figure 3. Examples of heat engines using Nitinol: (a) Offset crank engine; (b) Turbine engine; (c) Field engine (7)

Turbine engines utilize a single, continuous loop of Nitinol wire (usually in the form of tight helical coils) which is wound around a system of pulleys. Different portions of the loop are exposed to the high temperature bath or the low temperature bath. The difference in tension between the hot and cold portions of the loop causes a net torque to be applied to one of the pulleys. As this pulley rotates under the applied torque, it advances the loop through the complete heating and cooling cycle.

The field engines use the Nitinol to displace small masses such that a force field (gravitational, electric, or magnetic) can act on them and cause rotation. For example, in figure 3(c) small masses are connected together with Nitinol wire. As the Nitinol passes through the hot reservoir it contracts, thus increasing the mass density of the right side of the device. Conversely, as the Nitinol passes through the cold reservoir the Nitinol expands and reduces the mass density of the left side of the device. Hence, a greater gravitational attractive force is acting on the right side and, consequently, the loop travels in a clockwise direction.

Designs of the offset crank type have been patented by Banks (4), Hochstein (18), and Smith (21). Lee (20) and Johnson (19) have patents on turbine engine type designs. A field engine type design has been patented by Cory (17).

The best known operating low temperature Nitinol heat engine is that designed and built by Ridgway Banks (4) of Lawrence Berkeley Laboratory (see figure 4). His offset crank engine is about 13 inches

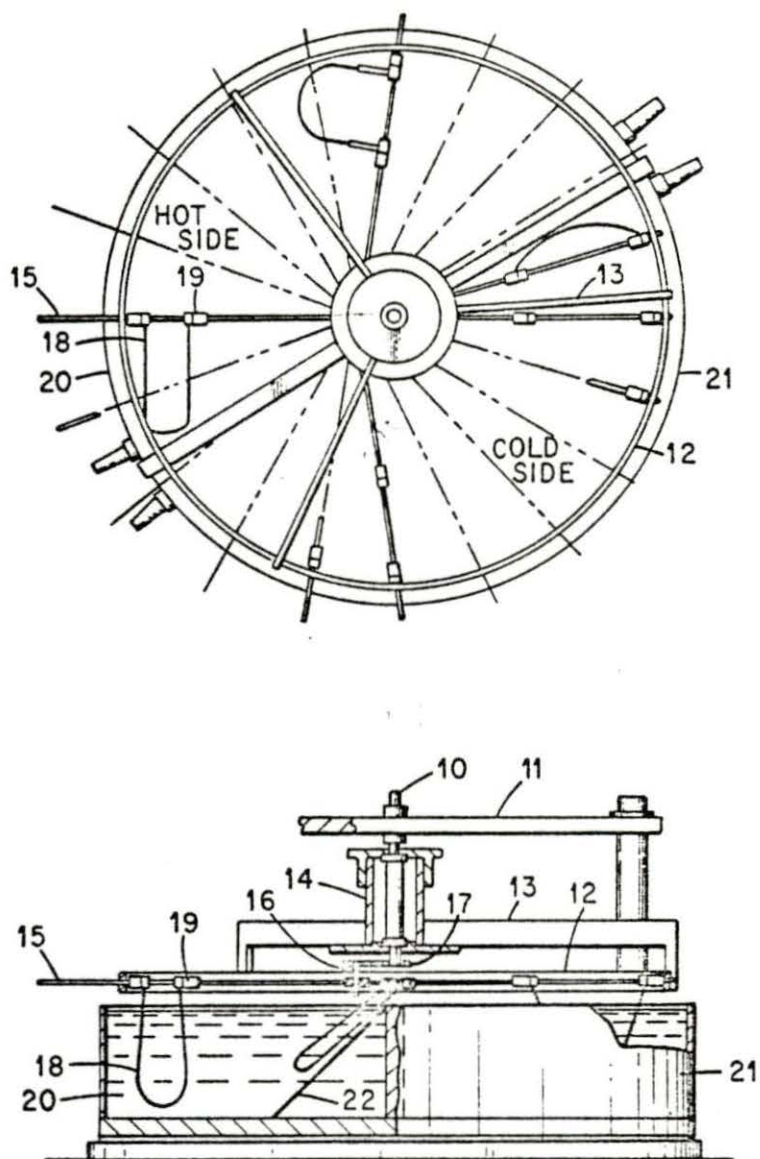


Figure 4. Top and side view of Banks' Nitinol heat engine (4)



in diameter, and uses twenty 12-inch long, 0.05 inch diameter wires. Each wire is bent into the shape of a "U" (also called loops). The wires have a straight memory configuration in the high temperature phase, and each provides a small tangential force on the rotating wheel as it attempts to return to this shape. The loops are carried around the circuit by the rotating outer wheel and thus they are alternately dipped into hot ( $T=48^{\circ}\text{C}$ ) and cold ( $T=24^{\circ}\text{C}$ ) water baths. The wires are forced to return to the loop shape while they are in the low temperature phase. Banks' engine operates at about 60 rpm and is estimated to develop a power of 0.2 watts (5,7).

## V. NEW LOW TEMPERATURE HEAT ENGINE DESIGN

The proposed new low temperature heat engine design is a modification of the Banks' engine (4) as suggested by Wechsler (24). This chapter undertakes the task of presenting a brief discussion on the design characteristics and principles of operation, a detailed account of its construction, an analytical determination of the expected work output, and a calculation of the power and efficiency to be expected from a prototype engine.

### A. Basic Design Characteristics and Principles of Operation

The engine, as shown in figure 5, is of the offset crank type. It embodies a number of spokes which contain straight Nitinol tubes. The spokes are pinned at one end to a fixed outer rim and at the other end attached, through a spring, to an offset crank. The tubes are straight at all times rather than bent so that all of the force developed by the Nitinol elements upon transformation is delivered to the crank. In this way, less shape memory material is required for the same amount of transformation-produced displacement.

The Nitinol tubes will be trained such that they have two-way memory. Upon transformation to the low temperature phase, each tube's length increases by an amount  $\Delta L$  over the length  $L_T$  it had in the high temperature phase. Conversely, upon reverse transformation to the high temperature phase the tube will return to its initial length. The change in tube length, as a result of transformation, changes the

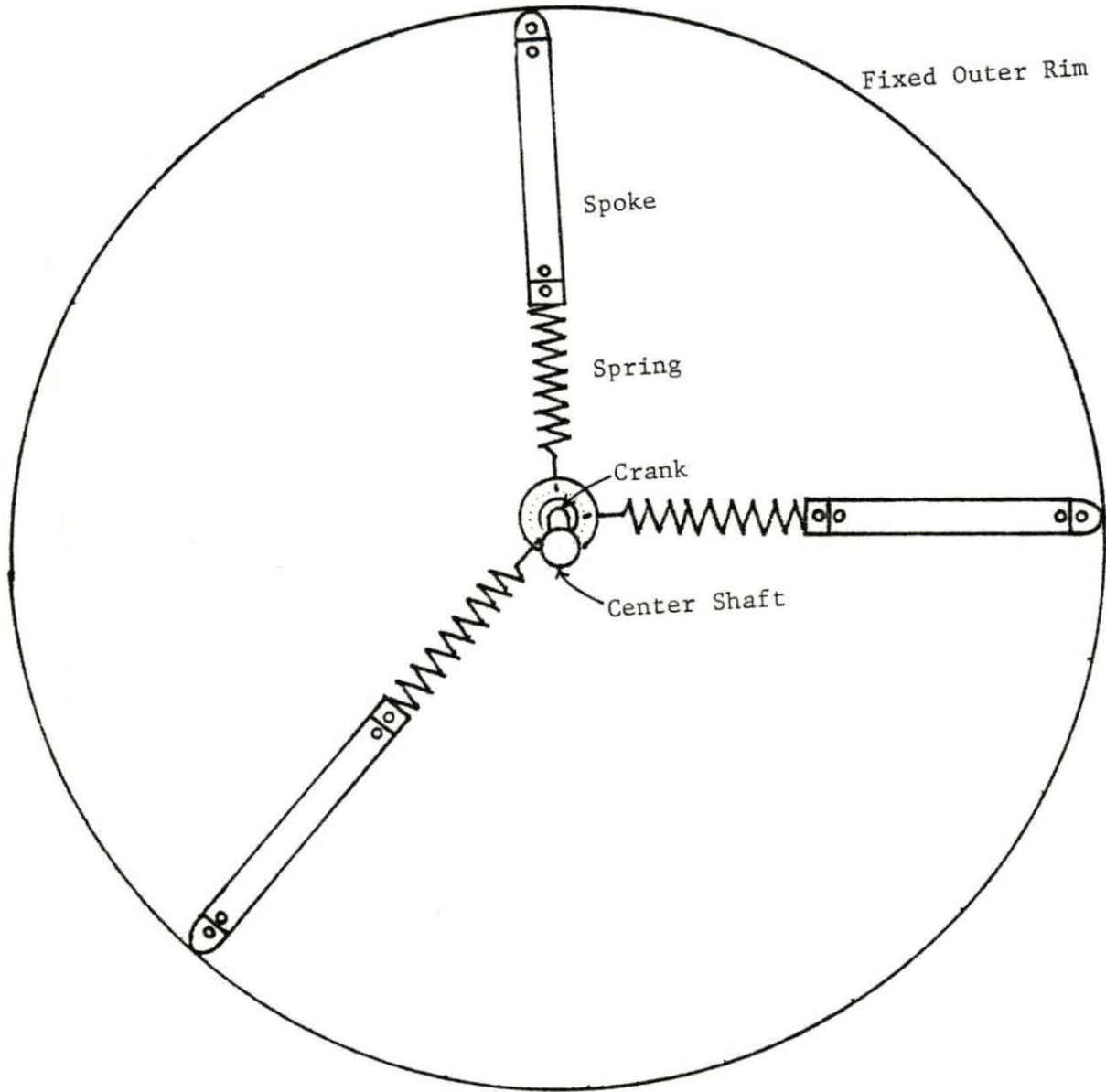


Figure 5. General layout and major components of proposed Nitinol heat engine

extension of the spring to which it is attached. This change in spring extension is felt by the crank, inasmuch as the spring can be considered a linear displacement-force converter, as a change in the force applied to it by that spoke. The force, acting on the crank, applies a moment on the center shaft through the offset distance moment arm, thus causing rotation.

The heat energy that the tubes use for transformation to the high temperature phase is delivered by a fluid, at a temperature greater than that required for transformation, flowing through the inside of the tube. Cold fluid flowing around the outside of the tube causes the tube to revert back to the low temperature phase. The hot and cold fluid flows are controlled so as to allow the greatest amount of work output for a given temperature induced displacement.

It should be noted that the concept of using Nitinol tubes as the working element in a heat engine was first proposed by Wechsler and Banks in 1977 (25). The advantage of using tubes in a heat engine is that the hot and cold fluids may be kept totally separated and thus, the problems associated with intermixing are avoided.

#### B. Construction Details

The fixed outer rim is a steel bar, of rectangular cross section, which has been rolled into a large circle and its ends joined by welding. The use of a fixed outer rim (rather than a rotating rim) simplifies the placement of the required auxiliary components (e.g.

valves and valve operators) which may be arranged around the periphery of the rim.

Each spoke (figure 6) is attached to the outer rim through a steel end piece. The end piece is pin connected to the rim at points equally spaced around the rim's circumference. The angular displacement between each pinned connection is 15 degrees with respect to the center of the circle defined by the outer rim. The pins used to connect the end piece to the rim allow the spokes to move in the plane of the circle formed by the outer rim with very little resistance. The end piece also provides an inlet nozzle so that hot water (for half of the cycle) and compressed air (for the other half) may enter the Nitinol tube.

The Nitinol tube has pipe threads machined at each end on its outer surface so that it may be screwed into the upper end piece (the threads also allow the lower end piece to be screwed onto the tube). Surrounding the tube is a steel outer jacket, through which cold water and compressed air may flow alternately around the Nitinol element. The steel jacket contains inlet and outlet ports for the cold water and air. It is attached to the upper end piece by welding, and to the lower end piece through a sliding fit.

The lower steel end piece has an outlet nozzle for the hot water and air. It is screwed onto the Nitinol tube by means of pipe threads machined on a portion of its interior surface. The lower end piece also has a groove cut around its outer cylindrical surface so that it can hold a teflon seal over which the outer jacket's lower end may

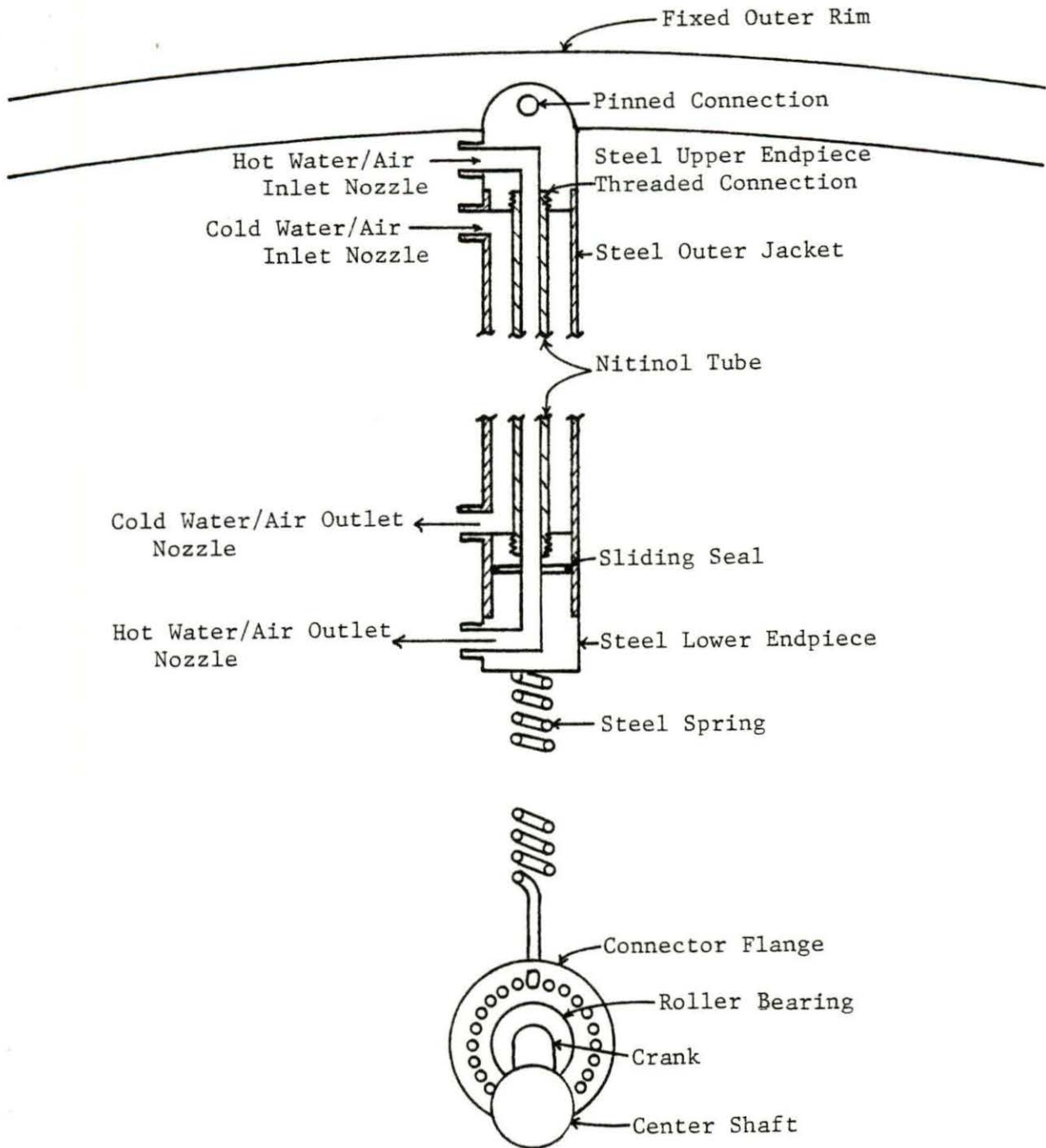


Figure 6. Cutaway view of one spoke in proposed Nitinol heat engine

slide as the Nitinol tube expands and contracts during the course of a cycle. The purpose of the seal is to prevent the cold water or air from leaking out of the annulus between the jacket's inner surface and the tube's outer surface.

Welded to the bottom of the lower end piece is the first coil of a steel helical spring. The opposite end of the spring is formed into a hook, which can be slipped through one of the holes in the connector flange. The hook acts like a pinned connection to allow for the wobbling motion of the spoke, which takes place as the crank goes through a cycle, without providing a great deal of resisting torque to the spoke.

The steel connector flange has 24 equally spaced holes drilled through its flat faces. The holes are also located equidistant from the flange's inner and outer diameters. The inner circular surface of the connector flange is welded to the outer race of a steel roller bearing (figure 7). The roller bearing's inner race is attached to the outer diameter of the crank through an interference fit. The crank is rigidly attached to the center shaft.

Figure 7 illustrates the proposed method by which more of the heat energy contained in the high temperature fluid may be extracted. A second wheel identical to the first is mounted on the same crank arm. The Nitinol tubes in the spokes of the second wheel would be of such a nickel-titanium composition so as to have a slightly lower phase transformation temperature than the tubes in the first wheel. During operation of the device three-way valves, located around the perimeter of the outer rim, feed hot water and compressed air alternately through

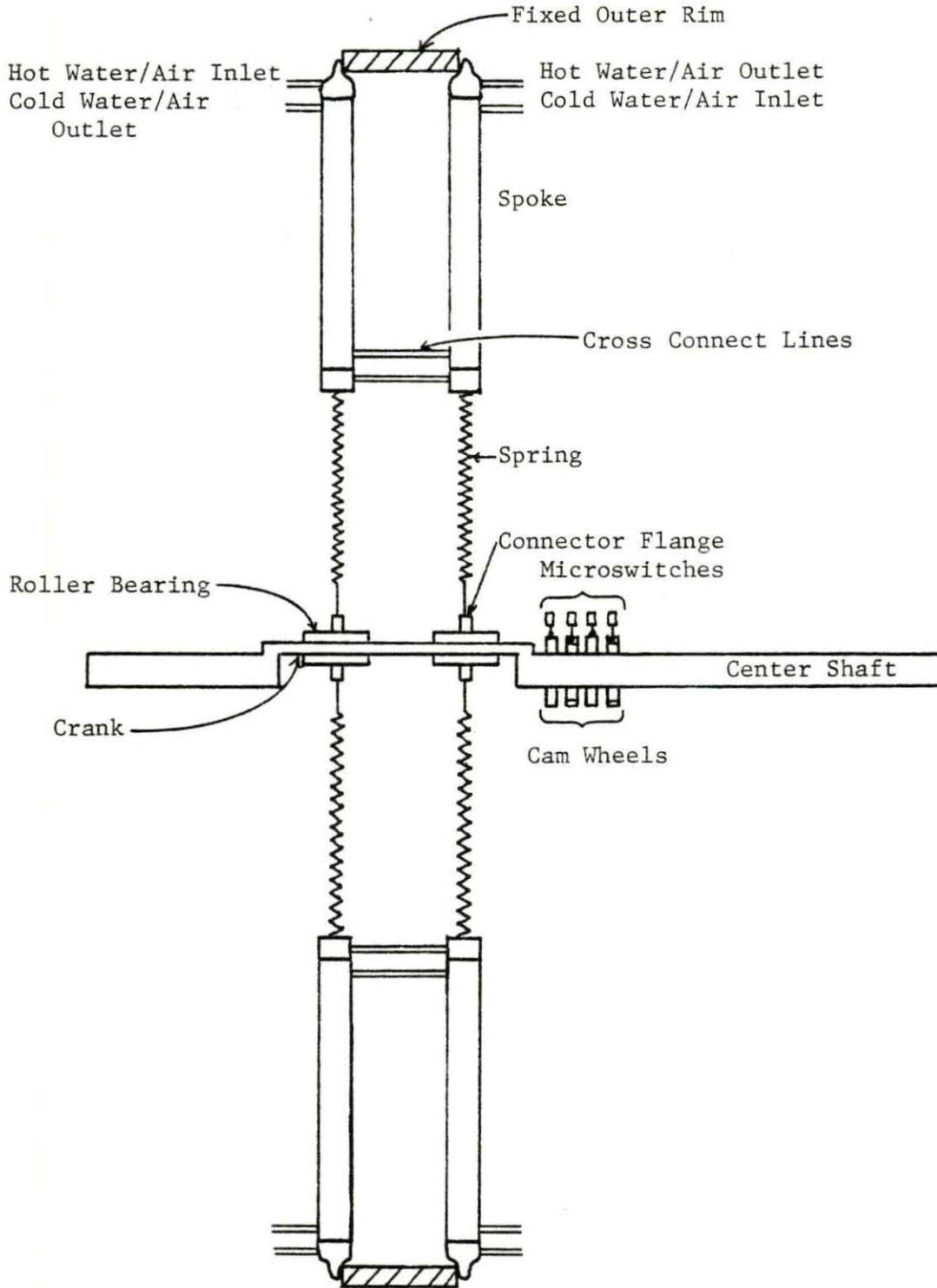


Figure 7. Side view of proposed two-wheel Nitinol heat engine



the Nitinol tubes in the left-hand wheel (figure 7) and out through the tubes in the right-hand wheel. At the same time, air and cold water flow alternately into the steel jackets on the right-hand wheel spokes, fed by similar three-way valves. Each spoke in one wheel is supplied with the hot water or air by one valve and with cold water or air by another valve. The three-way inlet valves are each connected to either a hot water or cold water upstream header as well as to a compressed air header. The return lines from each wheel contain three-way valves beyond which the lines are connected to appropriate hot or cold water headers. In the case of air flow, the outlet valves vent the air to the atmosphere in order to minimize water loss and the amount of air introduced into the water systems. Since the two wheels would be rotating at the same speed, the cross connection lines between the wheel assemblies would not need to be flexible.

Timing the flow of water or air so that each tube transforms at the appropriate time in the cycle would be accomplished through the use of cam wheels mounted on the center shaft. The cam wheels rotate with the shaft and actuate microswitches at various times throughout the cycle. The microswitches in turn send signals to the valve operators (e.g., solenoid coils) so that hot (cold) water or air is directed through (around) the Nitinol tube in a particular spoke at the proper time in the cycle. The attachment of the cams on the center shaft is such that each cam wheel can be adjusted relative to the position of the crank in the cycle. This allows for the timing of the hot and

cold fluid flows as deemed necessary in order to achieve the greatest work output.

### C. Analytical Determination of Work Output

A simplified version of the proposed engine design is shown in figure 8. This model is composed of a single spoke connected to the crank. The purpose here is to determine an expression for the expected net work output from one spoke in a single cycle.

The point A (figure 8) indicates the crank's position when the Nitinol tube in the spoke transforms from the high temperature phase to the low temperature phase. The crank will occupy the position designated B when the reverse transformation takes place.

The radius of the wheel  $r_w$ , the radius of the circle described by the crank as it completes a cycle  $r_c$ , and the length of the spoke when the crank is at position  $\theta$ ,  $L_s(\theta)$ , can all be put in vector notation:

$$\vec{r}_w = r_w \bar{j} \quad (5.1)$$

$$\vec{r}_c(\theta) = r_c \sin\theta \bar{i} + r_c \cos\theta \bar{j} \quad (5.2)$$

$$\vec{L}_s(\theta) = -r_c \sin\theta \bar{i} + (r_w - r_c \cos\theta) \bar{j} \quad (5.3)$$

where  $\bar{i}$  and  $\bar{j}$  designate unit vectors along the x- and y-axis respectively.

The total spoke length  $L_s(\theta)$  is also the sum of the lengths of the endpieces  $L_R$ , the tube  $L_T(\theta)$ , and the spring  $L_k(\theta)$ . Hence,

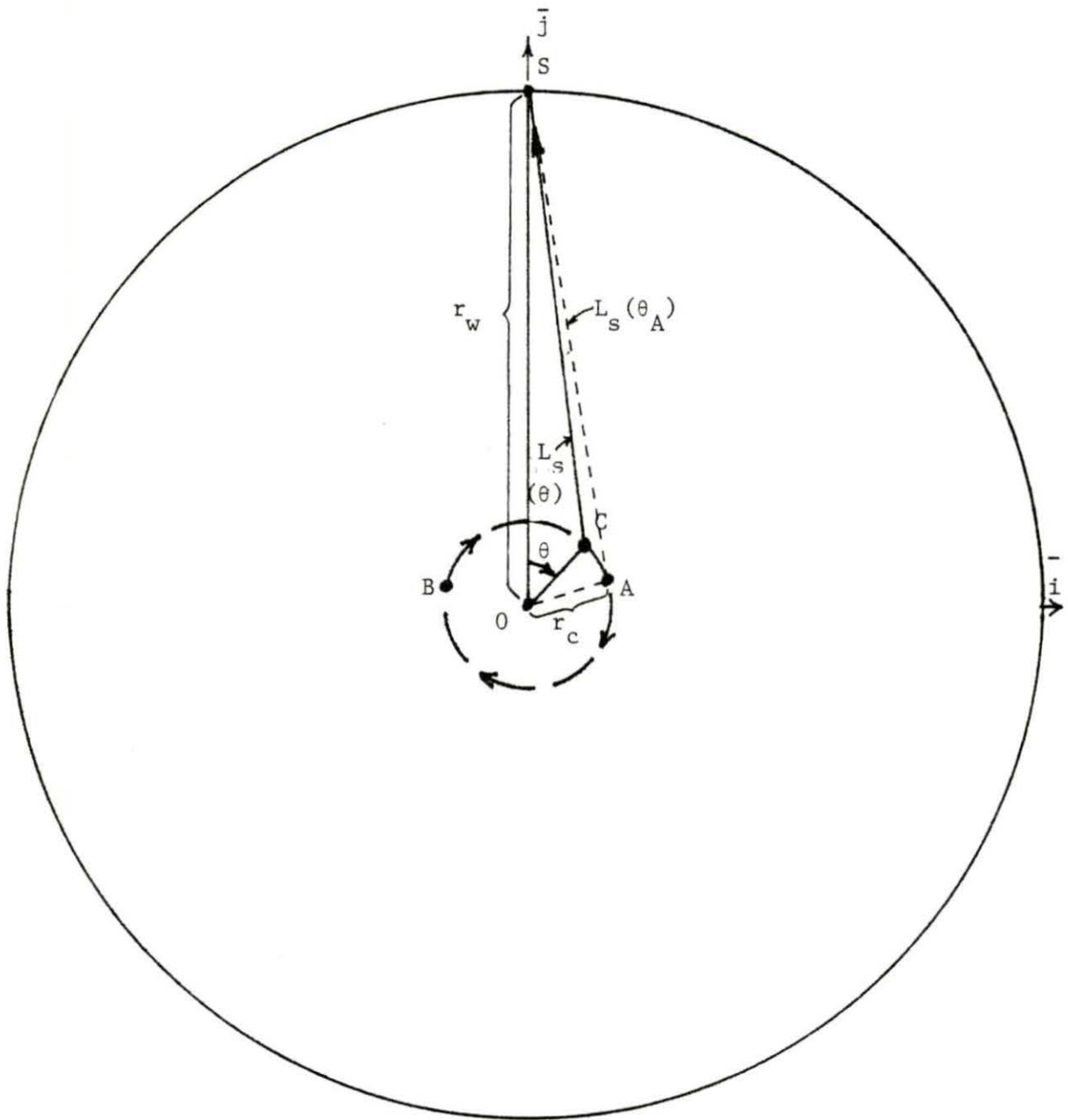


Figure 8. Arrangement of spoke, crank, and wheel for single spoke Nitinol heat engine

$$\vec{L}_s(\theta) = [L_R + L_T(\theta) + L_K(\theta)]\bar{i}_s, \quad (5.4)$$

where

$$L_T(\theta) = \begin{cases} L_T, & 0 \leq \theta \leq \theta_A \\ L_T + \Delta L, & \theta_A \leq \theta < \theta_B \\ L_T, & \theta_B \leq \theta < 2\pi \end{cases} \quad (5.5)$$

and  $\bar{i}_s$  is a unit vector lying along the direction of  $\vec{L}_s(\theta)$

$$\begin{aligned} \bar{i}_s &= \frac{\vec{L}_s(\theta)}{L_s(\theta)} \\ &= \frac{1}{L_s(\theta)} \{r_c \sin\theta \bar{i} + (r_w - r_c \cos\theta) \bar{j}\} \end{aligned} \quad (5.6)$$

$$L_s(\theta) = \{r_c^2 + r_w^2 - 2r_c r_w \cos\theta\}^{1/2} \quad (5.7)$$

The length of the spring  $L_K(\theta)$  can be expressed as the sum of its unloaded length  $L_o$  and the amount of extension over  $L_o$  that the spring experiences when the crank is rotated to  $\theta$  radians, thus

$$L_K(\theta) = L_o + L_e(\theta). \quad (5.8)$$

The force acting on the end of the crank arm is

$$\vec{F}(\theta) = kL_e(\theta). \quad (5.9)$$

From equations (5.4) and (5.8),

$$\vec{L}_s(\theta) = [L_R + L_T(\theta) + L_o + L_e(\theta)]\bar{i}_s \quad (5.10)$$

solving equation (5.10) for  $\vec{L}_e(\theta)$  yields

$$\vec{L}_e(\theta) = [L_s(\theta) - L_R - L_T(\theta) - L_o] \bar{i}_s \quad (5.11)$$

By substituting equation (5.11) into equation (5.9)

$$\vec{F}(\theta) = K[L_s(\theta) - L_R - L_T(\theta) - L_o] \bar{i}_s \quad (5.12)$$

The moment that  $\vec{F}(\theta)$  exerts on the crank is the cross product of the moment arm vector  $\vec{r}_c(\theta)$  and the applied force  $\vec{F}(\theta)$ ,

$$\vec{M}(\theta) = \vec{r}_c(\theta) \times \vec{F}(\theta). \quad (5.13)$$

Using equations (5.2) and (5.12) and by performing the vector product operation

$$\vec{M}(\theta) = \frac{K}{L_s(\theta)} [L_s(\theta) - L_R - L_T(\theta) - L_o] (r_c r_w \sin\theta) \bar{k} \quad (5.14)$$

where  $\bar{k}$  is a unit vector normal to the plane defined by the vectors  $\bar{i}$  and  $\bar{j}$  in the direction defined by the cross product  $\bar{i} \times \bar{j}$ . Equation (5.14) can be rearranged to yield

$$\vec{M}(\theta) = r_c r_w K \left[ \sin\theta - \frac{[L_R + L_T(\theta) + L_o] \sin\theta}{\{r_c^2 + r_w^2 - 2r_c r_w \cos\theta\}^{1/2}} \right] \bar{k} \quad (5.15)$$

The work done by the moment in a cycle is

$$W_1 = \oint \vec{M}(\theta) \cdot d\vec{\theta} \quad (5.16)$$

where  $\theta$  increases in a clockwise sense and leads to an additional negative sign. If the region of integration is divided into three parts bounded by  $\theta = 0$ ,  $\theta = \theta_A$ , and  $\theta = \theta_B$ , and the values for  $L_T(\theta)$  from equation (5.5) are substituted into equation (5.16), then the work done in a cycle is

$$\begin{aligned}
W_1 = & \int_0^{\theta_A} r_c r_w K \left[ \frac{(L_R + L_T + L_o) \sin\theta}{\{r_c^2 + r_w^2 - 2r_c r_w \cos\theta\}^{1/2}} - \sin\theta \right] d\theta \\
& + \int_{\theta_A}^{\theta_B} r_c r_w K \left[ \frac{(L_R + L_T + \Delta L + L_o) \sin\theta}{\{r_c^2 + r_w^2 - 2r_c r_w \cos\theta\}^{1/2}} - \sin\theta \right] d\theta \\
& + \int_{\theta_B}^{2\pi} r_c r_w K \left[ \frac{(L_R + L_T + L_o) \sin\theta}{\{r_c^2 + r_w^2 - 2r_c r_w \cos\theta\}^{1/2}} - \sin\theta \right] d\theta. \quad (5.17)
\end{aligned}$$

Performing the integration gives

$$W_1 = K\Delta L \left[ \{r_c^2 + r_w^2 - 2r_c r_w \cos\theta_B\}^{1/2} - \{r_c^2 + r_w^2 - 2r_c r_w \cos\theta_A\}^{1/2} \right] \quad (5.18)$$

Note that  $W_1$  in equation (5.18) has its greatest positive value when  $\theta_A = 0$  and  $\theta_B = \pi$  radians. Substituting these values into equation (5.18) results in

$$W_1 = 2K\Delta L r_c \quad (5.19)$$

as the net work done by a single Nitinol tube in a cycle.

An alternative method of determining the net work done by a tube in one cycle is presented in Appendix A. The viewpoint in that calculation is that the work done by the Nitinol tube on the spring equals the work done on the crank in the cycle.

#### D. Estimated Performance

Performance estimation requires the selection and optimization of design parameters which in turn necessitates the development of design

equations. In this section the general design equations for the proposed new heat engine are determined, and are then applied to the case of a prototype in order to determine its dimensions, and expected power output and efficiency.

### 1. Pertinent design equations

The physical dimensions of the Nitinol tubes, the springs, the wheel radius, and the crank offset distance are interconnected in such a way that once one parameter is chosen the other component dimensions are determined (or are required to fall within a specified range).

The cross sectional area of the tube is limited by the maximum allowable stress

$$A_T^c = \frac{F(\theta)}{\sigma_T}, \quad (5.20)$$

where the maximum  $\sigma_T$  is specified to be no greater than the yield stress of the tube  $\sigma_{ys}^T$  when it is in the low temperature phase. It can be seen from equations (5.7) and (5.12) that this extreme condition will occur at  $\theta = \pi$  radians.

The low temperature phase Nitinol tube length,  $L_T + \Delta L$ , is related to the cross sectional area and mass  $M_T$  through the following relation

$$L_T + \Delta L = \frac{M_T}{A_T^c \rho_N} \quad (5.21)$$

where  $\rho_N$  is the density of the Nitinol as given in table 1, and where

$$\Delta L = \epsilon L_T, \quad (5.22)$$

in which  $\epsilon$  is the transformation strain exhibited by the tube. The Transformation strain is assumed to be  $0.08 \frac{\text{in}}{\text{in}}$ , the experimentally determined strain which accompanies the greatest restoring force in Nitinol (3).

From equation (5.12) the magnitude of the applied force is

$$F(\theta) = K[L_S(\theta) - L_R - L_T(\theta) - L_O].$$

Splitting  $L_O$  into the length of the coiled portion of the spring  $L_C$  plus the length of the hook  $L_H$ , and substituting for  $L_O$  in the above equation gives

$$F(\theta) = K[L_S(\theta) - L_R - L_T(\theta) - L_C - L_H]. \quad (5.23)$$

Additionally, the coiled length of the spring can be approximated as

$$L_C \approx DN, \quad (5.24)$$

where  $N$  is the number of coils in the spring and  $D$  is the diameter of the spring wire. In order to ensure that there is an adequate length of coiled spring to stretch a total distance of  $2r_c$ ,  $L_C$  will be required to satisfy the following:

$$L_C \geq 4r_c. \quad (5.25)$$



The spring constant  $K$  (also called the spring modulus) can be calculated using the following equation (26)

$$K = \frac{GD^4}{64NR^3} \quad (5.26)$$

in which  $G$  is the modulus of rigidity of the spring material, and  $R$  is the mean radius of the spring coil. Another relationship to be considered in the design of the spring is the spring index  $C$ , which is a measure of the relative curvature of the coil,

$$C = \frac{2R}{D}. \quad (5.27)$$

It is usually specified (27) that

$$3 \leq C \leq 10 \quad (5.28)$$

because it is more difficult to accurately coil springs that have a very large or very small spring index. The spring must also be designed so that when at its greatest extension in the cycle (i.e.,  $\theta = \pi$ ) it will not exceed its own yield stress. The nature of helical springs is such that the limiting condition for the spring is the shear stress  $\tau$  it is under at the yield point, thus

$$\tau_{\max}^s = \tau_{ys}^s = \frac{1}{2} \sigma_{ys}^s, \quad (5.29)$$

where  $\sigma_{ys}^s$  is the yield stress of the spring material. The relationship between the shear stress on the spring and the load it is under is given by (26)

$$\tau_s = \frac{16F(\theta) R}{\pi D^3} \left[ \frac{4C-1}{4C-4} + \frac{(1+2\nu_s)}{2(1+\nu_s)C} \right] \quad (5.30)$$

where  $\nu_s$  is Poisson's ratio for the spring material and the bracketed quantity is the effect of the spring's curvature on  $\tau_s$ .

Figure 9 shows that near the connector flange the distance between adjacent spring coils is very small. In order to prevent one spring from interfering with the motion of its neighbor, it is required that the mean spring coil radius satisfies the following

$$\begin{aligned} R &= Z \tan 7.5^\circ - \frac{D}{2} \\ &= 0.13Z - \frac{D}{2}, \end{aligned} \quad (5.31)$$

where  $Z$  is the mean distance from the center of the crank arm to the nearest coil of the spoke at  $\theta = 0$ .

Finally, the relationship between  $r_c$ ,  $r_w$ , and  $L_s(\theta)$  is given by equation (5.7), which for  $\theta = 0$ , yields

$$L_s = r_w - r_c,$$

and for  $\theta = \pi$

$$L_s = r_w + r_c.$$

However, because of the presence of the connector flange (assumed to be 2 inches in diameter) with the hook holes located 0.25 inches from the

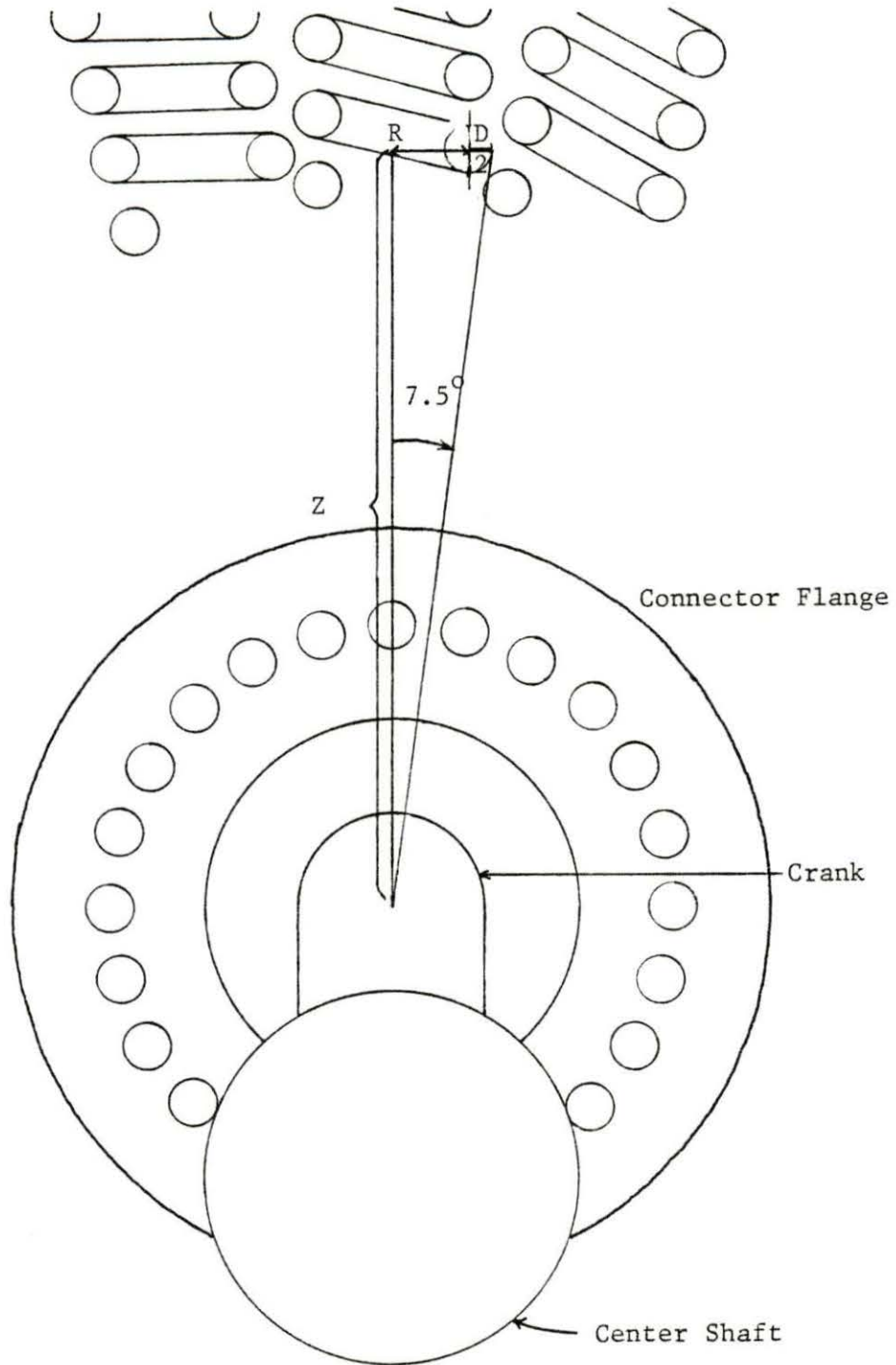


Figure 9. Determination of distance between center of crank and spring coil

outer circumference, the actual values of  $L_s$  at  $\theta = 0$  and  $\theta = \pi$  are

$$L_s(0) = r_w - r_c - 0.75, \quad (5.32)$$

$$L_s(\pi) = r_w + r_c - 0.75. \quad (5.33)$$

## 2. Determination of component dimensions

The design of a heat engine depends on the applications for which it is intended and the power rating chosen as a standard. For example, a heat engine designed to recover a portion of the very large amount of waste heat rejected from a power plant would necessarily be much larger and more complex than one designed to recover the very much smaller amount of heat made available from an unfocused solar heat collector.

Ginell et al. (16) claim that one kilowatt of power can be obtained from a device using one kilogram of Nitinol. For that reason, one kilogram has been arbitrarily selected as the mass of Nitinol to be used in this prototype model. Additionally, the prototype will incorporate the dual-wheel offset crank concept (figure 7), hence each wheel will utilize 0.5 Kg of Nitinol. Since each wheel is composed of 24 equally spaced spokes, each spoke then contains a Nitinol tube of mass  $M_T$ , where

$$\begin{aligned} M_T &= \frac{0.5\text{Kg}}{24} \left( 2.2 \frac{\text{lbm}}{\text{Kg}} \right) \\ &= 4.6 \times 10^{-2} \text{ lbm Nitinol} \end{aligned} \quad (5.34)$$

The engine design as implied by equations (5.20) through (5.34) involve 17 unknown parameters. As the equations show, these parameters are interrelated and examination reveals that in addition to specifying the mass of Nitinol to be used, three additional values must be selected more or less arbitrarily. The three parameters chosen to be specified in this way are  $L_R$ ,  $L_H$ , and  $Z$ . These particular terms were selected because it appears that they are relatively insensitive to the application of interest and to changes in engine application. The values given to these three parameters are

$$L_R = 2 \text{ inches} \quad (5.35)$$

$$L_H = 1.25 \text{ inches} \quad (5.36)$$

$$Z = 2 \text{ inches} \quad (5.37)$$

Mohamed (14) indicates that the yield stress for low temperature phase Nitinol is 5692 psi. The material of the spring is assumed to be cold worked stainless steel with the following mechanical properties (28):

$$G = 12.5 \times 10^6 \text{ psi}$$

$$\sigma_{ys}^s = 1.65 \times 10^5 \text{ psi}$$

$$\nu_s = 0.3.$$

Using these values and those given in equation (5.35) through (5.37) in the design equations (from section 1) to solve for the remaining

unknown parameters yields the results listed in table 2. The calculations are given in Appendix B.

Table 2. Wheel design parameters (based on 0.5 kg Nitinol per wheel)

Symbol	Parameter	Value	Units
$A_T^C$	Cross sectional area of tube	$2.0 \times 10^{-2}$	sq. in.
C	Spring index	3	(dimensionless)
D	Spring wire diameter	0.13	in.
$F(\pi)$	Maximum load on spring	113.0	lbf
K	Spring constant	154.8	lbf/in.
$L_c$	Length of spring coil	5.85	in.
$\Delta L$	Transformation displacement of tube	0.73	in.
$L_T$	Length of tube (HTP)*	9.10	in.
N	Number of coils in spring	45	(dimensionless)
R	Mean spring coil radius	0.20	in.
$r_c$	Crank offset distance	0.73	in.
$r_w$	Wheel radius	19.70	in.

\* High temperature phase

### 3. Calculation of expected work, power, and efficiency

As shown by equation (5.19) the work done by one tube during the course of a cycle is

$$W_1 = 2K\Delta Lr_c.$$

Using the values given in table 2 for a 0.5 Kg Nitinol wheel,

$$\begin{aligned}
 W_1 &= 2(154.8 \frac{\text{lb}_f}{\text{in}})(0.73 \text{ in})^2 \\
 &= 165 \text{ in-lbf} \\
 &= 13.7 \text{ ft-lbf.}
 \end{aligned}$$

The total work done by all 24 tubes in the wheel during a cycle is then

$$\begin{aligned}
 W &= 24 W_1 \\
 &= 24 (13.7 \text{ ft-lbf}) \\
 &= 328.8 \text{ ft-lbf} \qquad (5.38)
 \end{aligned}$$

Since power is the rate of doing work, a determination of the speed at which the prototype operates must be made. The limiting factor is the rate at which enough heat can be transferred to the tube material in order to cause transformation to the high temperature phase. Appendix C contains the calculation for the time it takes for the tube to transform once hot water at 115<sup>o</sup>F is introduced into the tube. The heating half-cycle time is found to be about one second, thus the total cycle time will be 2 seconds. In this case the power output of the wheel is then

$$\begin{aligned}
 P_1 &= \frac{W}{t} \\
 &= \frac{(328.8 \text{ ft-lbf})(0.7457 \text{ Kw/hp})}{(2 \text{ sec})(550 \frac{\text{ft-lbf}}{\text{hp-sec}})} \\
 &= 0.22 \text{ Kw.}
 \end{aligned}$$

and for the dual-wheel system the total power is twice this value

$$\begin{aligned}
 P &= 2P_1 \\
 &= 0.44 \text{ Kw.}
 \end{aligned}$$

The resulting power-to-Nitinol mass ratio is

$$\begin{aligned}
 \frac{P}{48M_T} &= \frac{0.44 \text{ Kw}}{1.0 \text{ Kg}} \\
 &= 0.44 \text{ Kw/Kg.}
 \end{aligned}$$

This is less than half the value predicted by Ginell et al. (16). The same ratio for the Banks engine (5) is

$$\begin{aligned}
 \frac{P}{20 M_N} &= \frac{2 \times 10^{-4} \text{ Kw}}{20(30 \text{ cm}) \frac{\pi}{4} (0.12 \text{ cm})^2 (0.234 \frac{\text{lbm}}{\text{in}^3}) (\frac{1 \text{ in}}{2.54 \text{ cm}})^3 (\frac{0.454 \text{ Kg}}{\text{lbm}})} \\
 &= 4.6 \times 10^{-3} \text{ Kw/Kg}
 \end{aligned}$$

or about 1% of the value obtained for this prototype.

From Appendix C, the amount of heat delivered to a tube in the course of a cycle is



$$Q_1 = 1.12 \text{ Btu.}$$

The total amount of heat delivered to one wheel during a cycle is then

$$\begin{aligned} Q &= 24 Q_1 \\ &= 24 (1.12 \text{ Btu}) \\ &= 26.9 \text{ Btu} \end{aligned} \tag{5.39}$$

An engine's efficiency is defined to be the ratio of the net work output to the total heat input, thus using the values given in equations (5.38) and (5.39) the prototype's efficiency  $\eta$  is

$$\begin{aligned} \eta &= \frac{W}{Q} \times 100\% \\ &= \frac{328.8 \text{ ft-lbf}}{(26.9 \text{ Btu}) \left(778 \frac{\text{ft-lbf}}{\text{Btu}}\right)} \times 100\% \\ &= 1.6\% \end{aligned}$$

The Carnot efficiency is given by

$$\eta_c = \frac{T_H - T_L}{T_H} \times 100\%$$

where  $T_H$  and  $T_L$  are the temperatures of the heat source and heat sink given on the absolute temperature scale

$$T_H = 115^{\circ}\text{F} + 460$$

$$= 575^{\circ}\text{R}$$

$$T_L = 35^{\circ}\text{F} + 460$$

$$= 495^{\circ}\text{R}.$$

Hence,

$$\eta_c = \frac{575^{\circ}\text{R} - 495^{\circ}\text{R}}{575^{\circ}\text{R}} \times 100\%$$

$$= 13.9\%$$

and thus the prototype's efficiency is about 11% of the Carnot efficiency.

VI. APPLICATION TO WASTE HEAT UTILIZATION IN  
ELECTRIC GENERATING POWER PLANTS

The reactor of Unit #1 at the Prairie Island nuclear power plant is rated at 1650M<sub>w</sub> thermal power. It is designed to discharge  $3.9 \times 10^9 \frac{\text{Btu}}{\text{hr}}$  (1143 MW<sub>t</sub>) at a maximum temperature of 107<sup>o</sup>F from its condenser at full power (29). If larger versions of the dual-wheel low temperature heat engine prototype are used to recover useful work from the heat rejected by the Prairie Island nuclear power plant, then at a conversion efficiency of 1.6% the total additional power output of the plant would be

$$\begin{aligned} P &= (0.016)(1143 \text{ Mw}) \\ &= 18.3 \text{ Mw.} \end{aligned}$$

Thus, the overall plant efficiency will be increased from 30.7% to 31.8%.

The mass of Nitinol required to convert the rejected heat into 18.3 Mw of additional power would be

$$\begin{aligned} M_{\text{NiTi}} &= \frac{18300 \text{ Kw}}{0.44 \text{ Kw/Kg}} \\ &= 41.6 \times 10^3 \text{ Kg Nitinol.} \end{aligned}$$

At a cost of \$60/Kg for Nitinol (16) this would amount to a capital cost of  $\$2.5 \times 10^6$  for the shape memory material alone. However, by selling the additional power generated at the price of 5.5 cents per Kw-hr

(30) the extra revenues after one year of operation would amount to about

$$(18300 \text{ Kw}) (\$0.055/\text{Kw-hr}) (8.6 \times 10^3 \frac{\text{hr}}{\text{yr}}) (1 \text{ yr})$$
$$= \$8.7 \times 10^6$$

Essentially, the cost of the Nitinol would be repaid after about four months of operation, with a net profit of  $\$6.2 \times 10^6$  going to the utility after the first year.

## VII. CONCLUSION

Despite the fact that the proposed heat engine design has a relatively low efficiency for the conversion of heat energy to useful mechanical energy, it does have the potential to provide several additional megawatts of electrical power from a single power plant without increasing the need for fossil or nuclear fuel. Also, because of the resistance of Nitinol to fatigue degradation (5), and because of the simplicity of its design such a device should not require very much in the way of maintenance or upkeep, thus it has the additional advantage of potentially low operating costs. Another advantageous feature of the new design is the ease with which additional wheels may be coupled in series with respect to the fluid flow thus enabling the extraction of a large percentage of the available heat energy by utilizing tubes with sequential transformation temperatures as suggested by Wechsler and Banks (25).

## VIII. REFERENCES

1. F. Golden, "The Energy Squeeze," "The American Peoples Encyclopedia Year Book 1974," (Grolier, New York, 1974), p.34.
2. D. M. Roberts and D. S. Bahr, Utilization of Waste Heat from Electric Power Generating Stations, Volume I, Final Report submitted to Iowa Energy Policy Council, Project 76-003-9, Department of Nuclear Engineering, Engineering Research Institute, Iowa State University, March 1978.
3. C. M. Jackson, H. L. Wagner, and R. J. Wasilewski, "55-Nitinol-- The Alloy with a Memory: Its Physical Metallurgy, Properties and Applications," NASA Report No. SP-5110 (1972).
4. R. M. Banks, "Energy Conversion System," U. S. Patent No. 3,913,326 (1975).
5. R. Banks, "Nitinol Heat Engines;" in Shape Memory Effects in Alloys, edited by J. Perkins (Plenum Press, New York, 1975).
6. J. P. Zmuda, "The Engine that Runs on Sunshine," Popular Science 204, 87 (1974).
7. W. S. Ginell, J. L. McNichols, Jr., and J. S. Cory, "Nitinol Heat Engines for Low-grade Thermal Energy Conversion," Mechanical Engineering 101, 28 (1979).
8. M. S. Wechsler and D. M. Roberts, "Shape-Memory Engines and Waste Heat Utilization," Iowa State University Research Proposal, 2-3 (1980).
9. C. L. Stong, "The Amateur Scientist," Scientific American 224, 118 (1971).
10. L. M. Schetky, "Shape-Memory Alloys," Scientific American 241, 74 (1979).
11. C. M. Wayman, "Some Applications of Shape-Memory Alloys," J. of Metals 32, 129 (1980).
12. Goodyear Aerospace Corp., "55-Nitinol Documentary Movie," SP-7000, (1969).
13. W. B. Cross, A. H. Kariotis, and F. J. Stimler, "Nitinol Characterization Study: Final Summary Report," NASA Report No. CR-1433 (1969).

14. H. A. E. Mohamed, "Martensite Transformation and Shape Memory Effect in Ni-Ti Alloy," Ph.D. thesis, Lawrence Berkeley Laboratory and University of California (1976).
15. D. T. Curry, "New Uses for Metals that Remember," Machine Design 51, 113 (1979).
16. W. S. Ginell, J. L. McNichols, W. P. Olson, and J. Cory, "Energy Conservation by Conversion of Low Temperature Heat Sources-- A White Paper," (McDonnell Douglas Astronautics Company-- West, Huntington Beach, CA, 1976).
17. J. S. Cory, "Variable Density Heat Engine," U.S. Patent No. 4,037,411 (1977).
18. P. A. Hochstein, "Thermal Energy Converting Assembly," U. S. Patent No. 4,037,411 (1977).
19. A. D. Johnson, "Memory Alloy Heat Engine and Method of Operation," U. S. Patent No. 4,055,955 (1977).
20. L. Lee II, "Motor," U. S. Patent No. 3,303,642 (1967).
21. W. K. Smith, "Compound Memory Engine," U. S. Patent No. 4,086,769 (1978).
22. "Industry Statistics," Oil and Gas Journal 78, 138 (1980).
23. W. J. Buehler and D. M. Goldstein, "Conversion of Heat Energy to Mechanical Energy," U. S. Patent No. 3,403,238 (1968).
24. M. S. Wechsler, "Rotary Shape Memory Heat Engine Using Shape Memory Tubes," 1980 (unpublished).
25. M. S. Wechsler and R. M. Banks, "Expanded-Thermal-Gradient Heat Engines Using Shape-Memory Material," Record of Invention, AEC Report No. IB-266 (1977).
26. A. D. Deutschman, W. J. Michels, and C. E. Wilson, Machine Design: Theory and Practice, (Macmillan, New York, 1975) pp. 721-724.
27. Springs: Materials, Design and Manufacture, (The Spring Research Association, Sheffield, England, 1968) p.3.
28. A. Higdon, E. H. Ohlsen, W. B. Stiles, J. A. Weese, and W. F. Riley, Mechanics of Materials, Third Edition (John Wiley and Sons, New York, 1960).

29. NSP Prairie Island Nuclear Generating Plant Final Safety Analysis Report, Vol. 1 (Northern States Power Company, Minneapolis, MN, circa, 1973).
30. Iowa Electric Light and Power Company Billing Statement (Iowa Light and Power Company, Boone, IA, 1980).
31. C. O. Bennett and J. E. Myers, Momentum, Heat, and Mass Transfer, Second edition (McGraw-Hill, New York, 1962).
32. R. H. Perry and C. H. Chilton, Chemical Engineers' Handbook, Fifth edition (McGraw-Hill, New York, 1973).



## IX. ACKNOWLEDGMENTS

The author wishes to thank Dr. Monroe Wechsler for the many hours spent in clarifying the shape memory phenomenon, formalizing the work equations, and for his recommendations of different design concepts. The author also wishes to express his gratitude to Dr. Donald Roberts who painstakingly pored over the initial draft of this manuscript and made numerous suggestions for its improvement, and to Miss Jo Sedore who faced the tedious task of typing this thesis with a smile. Finally, a special note of appreciation to my wife, Jackie, without whose love and understanding this work would not have been possible.

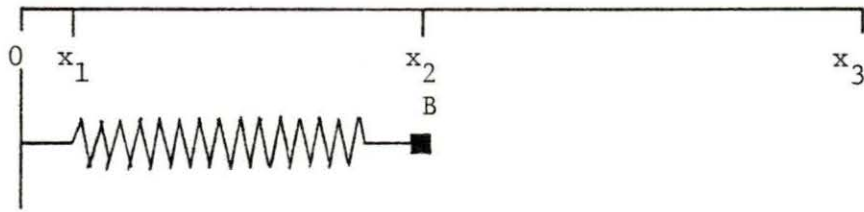
## X. APPENDIX A: CALCULATION OF WORK DONE BY TUBE

This appendix focuses on the spring contained in one of the spokes of the proposed low temperature heat engine design. The object here is to show analytically that the work done on the spring by the tube during transformation exactly equals the work done by the spring on some other external object (e.g., the crank arm of the proposed engine).

Figure 10 shows different configurations of a spring (with spring constant  $K$ ) which is attached at one end to a Nitinol tube and at the other end to the external object B. If B is constrained to move only along the  $x$ -axis and is massless, then figure 10(a) shows the spring in its unloaded condition with the end of the tube (in the high temperature phase) at  $x=0$  and B at  $x=x_2$ . In figure 10(b) the tube has transformed to the low temperature phase, thus extending its end to  $x=x_1$  while B is held at  $x=x_2$ ; figure 10(c) shows that B has moved to position  $x=x_3$ ; with B fixed at  $x=x_3$  the tube has retransformed to the high temperature phase in figure 10(d) and its end has returned to  $x=0$ ; figure 10(e) shows that B has been allowed to return to  $x=x_2$ , thus the system is again unloaded as in figure 10(a).

Work done by the tube on the spring occurs between steps (a) and (b), and between steps (c) and (d). As the tube end moves from  $x=0$  to  $x=x_1$  the force on the spring is

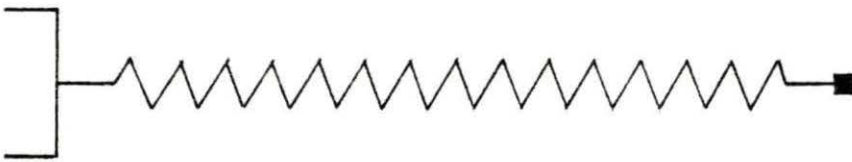
$$\begin{aligned} F_{ab} &= -K[(x_2-x) - (x_2-0)] \\ &= Kx. \end{aligned}$$



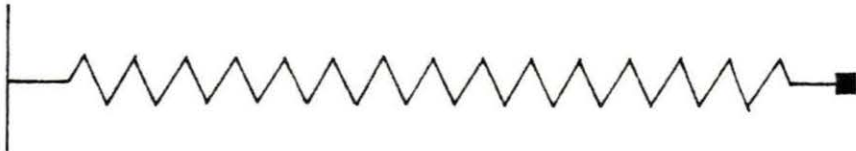
(a)



(b)



(c)



(d)



(e)

Figure 10. Simple model of spring motion during one cycle

The work done by the tube on the spring between steps (a) and (b) is then

$$\begin{aligned} W_{ab} &= \int_0^{x_1} F_{ab} \, dx \\ &= K \int_0^{x_1} x \, dx \\ &= 1/2Kx_1^2. \end{aligned}$$

As the tube moves from  $x=x_1$  to  $x=0$  the force on the spring is

$$\begin{aligned} F_{cd} &= -K[(x_3-x) - (x_2-0)] \\ &= -K[x_3-x-x_2], \end{aligned}$$

and the work done between steps (c) and (d) is

$$\begin{aligned} W_{cd} &= \int_{x_1}^0 F_{cd} \, dx \\ &= K \int_{x_1}^0 (x_3-x-x_2) \, dx \\ &= -K[0 - (x_3x_1 - 1/2x_1^2 - x_2x_1)] \\ &= K(x_3x_1 - 1/2x_1^2 - x_2x_1). \end{aligned}$$

The net work done by the tube on the spring is

$$\begin{aligned} W_{net} &= W_{ab} + W_{cd} \\ &= 1/2Kx_1^2 + Kx_3x_1 - 1/2Kx_1^2 - Kx_2x_1 \\ &= Kx_1(x_3 - x_2). \end{aligned}$$

When B is moved between steps (b) and (c), and steps (d) and (e) the force acting on B is

$$\begin{aligned} F_{bc} &= -K[(x-x_1) - (x_2-0)] \\ &= -K[x-x_1-x_2], \end{aligned}$$

and the work done is

$$\begin{aligned} W_{bc} &= \int_{x_2}^{x_3} F_{bc} dx \\ &= -K \int_{x_2}^{x_3} [x-x_1-x_2] dx \\ &= -K \left[ \frac{1}{2}x^2 - x_1x - x_2x \right]_{x_2}^{x_3} \\ &= -K \left[ \frac{1}{2}x_3^2 - x_1x_3 - x_2x_3 - \frac{1}{2}x_2^2 + x_1x_2 + x_2^2 \right] \\ &= -K \left[ \frac{1}{2}x_3^2 - x_1x_3 - x_2x_3 + \frac{1}{2}x_2^2 + x_1x_2 \right]. \end{aligned}$$

When B is moved between steps (d) and (e) the force is

$$\begin{aligned} F_{de} &= -K[(x-0) - (x_2-0)] \\ &= -K[x-x_2], \end{aligned}$$

while the work done is

$$\begin{aligned}
 W_{de} &= \int_{x_3}^{x_2} F_{de} dx \\
 &= -K \int_{x_3}^{x_2} (x-x_2) dx \\
 &= -K \left( \frac{1}{2} x^2 - x_2 x \right) \Big|_{x_3}^{x_2} \\
 &= -K \left[ \frac{1}{2} x_2^2 - x_2^2 - \frac{1}{2} x_3^2 + x_2 x_3 \right] \\
 &= -K \left[ -\frac{1}{2} x_2^2 - \frac{1}{2} x_3^2 + x_1 x_3 \right].
 \end{aligned}$$

The net work done by the spring on B is

$$\begin{aligned}
 W_{net} &= W_{be} + W_{de} \\
 &= -K[x_1 x_2 - x_1 x_3] \\
 &= Kx_1(x_3 - x_2).
 \end{aligned}$$

As can be seen this equals the net work done by the tube on the spring, and if it is noted that  $x_1 = \Delta L$  and  $(x_3 - x_2) = 2r_c$  then the net work done by the tube on the spring is

$$W = 2K\Delta L r_c;$$

which is the same as given in equation (5.19).

XI. APPENDIX B: CALCULATION OF PROTOTYPE  
COMPONENT DIMENSIONS

This appendix uses the design equations developed in Chapter V, Section C, to calculate the dimensions and other parameters for the Nitinol tubes, springs, crank, and wheel.

Equations (5.20) through (5.37) are reproduced below:

$$A_T^c = \frac{F(\theta)}{\sigma_T} \quad (5.20)$$

$$L_T + \Delta L = \frac{M_T}{A_T^c \rho_N} \quad (5.21)$$

$$\Delta L = \epsilon L_T \quad (5.22)$$

$$F(\theta) = K[L_S(\theta) - L_R - L_T(\theta) - L_C - L_H] \quad (5.23)$$

$$L_C \approx DN \quad (5.24)$$

$$L_C \geq 4r_c \quad (5.25)$$

$$K = \frac{GD^4}{64NR^3} \quad (5.26)$$

$$C = \frac{2R}{D} \quad (5.27)$$

$$3 \leq C \leq 10 \quad (5.28)$$

$$\tau_{\max}^s = \tau_{ys}^s = \frac{1}{2} \sigma_{ys}^s \quad (5.29)$$

$$\tau_s = \frac{16F(\theta) R}{\pi D^3} \left[ \frac{4C-1}{4C-4} + \frac{(1+2\nu)}{2(1+\nu)C} \right] \quad (5.30)$$

$$R = 0.13Z - \frac{D}{2} \quad (5.31)$$

$$L_s(0) = r_w - r_c - 0.75 \quad (5.32)$$

$$L_s(\pi) = r_w + r_c - 0.75 \quad (5.33)$$

$$M_T = 4.6 \times 10^{-2} \text{ lbm} \quad (5.34)$$

$$L_R = 2 \text{ in.} \quad (5.35)$$

$$L_H = 1.25 \text{ in.} \quad (5.36)$$

$$Z = 2 \text{ in.} \quad (5.37)$$

The mechanical properties of stainless steel, obtained from Higdon et al. (28), are also repeated

$$G = 12.5 \times 10^6 \text{ psi}$$

$$\sigma_{ys}^S = 1.65 \times 10^5 \text{ psi}$$

$$\nu_s = 0.3$$

as well as the value for the yield stress of low temperature phase Nitinol from Mohamed (14)

$$\sigma_{ys}^T = 5692 \text{ psi.}$$

The transformation strain as given in Jackson et al. (3) is



$$\epsilon = 0.08 \frac{\text{in}}{\text{in}}.$$

The method of calculating the values of the remaining unknown parameters is as follows: substituting equation (5.37) into equation (5.31) gives

$$\begin{aligned} R &= 0.13(2) - \frac{D}{2} \\ &= 0.26 - \frac{D}{2}, \end{aligned} \tag{B.1}$$

using this in equation (5.27) results in

$$\begin{aligned} C &= \frac{2[0.26 - \frac{D}{2}]}{D} \\ &= \frac{0.52 - D}{D} \\ &= \frac{0.52}{D} - 1, \end{aligned} \tag{B.2}$$

and solving equation (B.2) for D yields

$$D = \frac{0.52}{C+1}. \tag{B.3}$$

Choosing C=3 from equation (5.28) and back substituting into equations (B.3) and (B.1) gives

$$D = 0.13 \text{ in.} \tag{B.4}^*$$

$$R = 0.20 \text{ in.} \tag{B.5}^*$$

Solving equation (5.30) for F( $\theta$ ) gives

---

\*The values for the parameters shown in the equations designated by an asterisk are those listed in table 2.

$$F(\theta) = \frac{\tau_s \pi D^3}{16R} \frac{1}{\left[ \frac{4C-1}{4C-4} + \frac{1+2\nu}{2(1+\nu)C} \right]} \quad (\text{B.6})$$

and by substituting the values given in equations (B.4), (B.5), and (5.29) and using the given values for  $\sigma_{ys}^s$  and  $\nu_s$  yields the following result for  $F(\pi)$ :

$$F(\pi) = \frac{\frac{1}{2}(1.65 \times 10^5) \pi (0.13)^3}{16 (0.20)} \frac{1}{\left[ \frac{4(3)-1}{4(3)-4} + \frac{1+2(.3)}{2(1+.3)(3)} \right]}$$

$$= 113.0 \text{ lbf.} \quad (\text{B.7})^*$$

Similarly, for  $C = 10$ :

$$D = 0.05 \text{ in.}, \quad (\text{B.8})$$

$$R = 0.24 \text{ in.}, \quad (\text{B.9})$$

and

$$F(\pi) = 7.4 \text{ lbf.} \quad (\text{B.10})$$

The length of the tube in the prototype design will be minimized while at the same time allowing a larger force to act on the crank, hence the value chosen for  $C$  is

$$C = 3. \quad (\text{B.10a})^*$$

Substituting the value given for  $\sigma_{ys}^T$  and equation (B.7) into equation (5.20) gives

$$\begin{aligned}
 A_t^c &= \frac{113.0}{5692} \\
 &= 2.0 \times 10^{-2} \text{ in}^2
 \end{aligned}
 \tag{B.11)*}$$

Using this and equation (5.34) in equation (5.21) yields

$$\begin{aligned}
 L_T + \Delta L &= \frac{4.6 \times 10^{-2}}{(2.0 \times 10^{-2})(2.34 \times 10^{-1})} \\
 &= 9.83 \text{ in.},
 \end{aligned}
 \tag{B.12)}$$

and by substituting the value for  $\epsilon$  and equation (5.22) into equation (B.12) the result is

$$\begin{aligned}
 L_T + (0.08)L_T &= 9.83 \text{ in.} \\
 L_T &= \frac{9.83}{1.08} \\
 &= 9.10 \text{ in.}
 \end{aligned}
 \tag{B.13)*}$$

Subtracting equation (B.13) from equation (B.12) gives

$$\begin{aligned}
 L_T + \Delta L - L_T &= 9.83 - 9.10 \\
 \Delta L &= 0.73 \text{ in.}
 \end{aligned}
 \tag{B.14)*}$$

But, at  $\theta = \pi$  radians; prior to transformation to HTP for a single spoke:

$$F(\pi) = 113.0 \text{ lbf}$$

$$L_T(\pi) = 9.83 \text{ in.}$$

$$L_S(\pi) = r_w + r_c - 0.75$$

and by equation (5.23)

$$\begin{aligned} 113 &= K[r_w + r_c - 0.75 - 2 - 9.83 - L_c - 1.25] \\ &= K[r_w + r_c - 13.83 - L_c] \end{aligned} \quad (\text{B.15})$$

By similar means, at  $\theta=0$  radians; prior to tube transformation to LTP:

$$F(0) = 0$$

$$L_T(0) = 9.10 \text{ in.}$$

$$L_S(0) = r_w - r_c - 0.75,$$

then by equation (5.23)

$$\begin{aligned} 0 &= K[r_w - r_c - 0.75 - 2 - 9.10 - L_c - 1.25], \\ &= K[r_w - r_c - 13.10 - L_c] \end{aligned} \quad (\text{B.15a})$$

Adding equation (B.15a) to equation (B.15) gives

$$113 = K(2r_w - 26.93 - 2L_c), \quad (\text{B.16})$$

and subtracting equation (B.15a) from equation (B.15)

$$113 = K(2r_c - 0.73) \quad (\text{B.17})$$

However,  $K$  and  $r_c$  must be such that after the tube transforms at  $\theta=0$ ,  $F(0)$  will be

$$F(0) \leq 113 \text{ lbf}, \quad (\text{B.18})$$

but

$$F(0) = K\Delta L, \quad (\text{B.19})$$

so that by substituting equations (B.19) and (B.14) into equation (B.18) and solving for K yields

$$\begin{aligned} K &= \frac{113}{.73} \\ &= 154.8 \text{ lbf/in.} \end{aligned} \quad (\text{B.20})^*$$

Using equation (B.20) in equation (5.26) and solving for N gives

$$\begin{aligned} N &= \frac{(12.5 \times 10^6)(.13)^4}{64(154.8)(.2)^3} \\ &= 45 \text{ coils,} \end{aligned} \quad (\text{B.21})^*$$

then by equation (5.24)

$$\begin{aligned} L_c &\approx (0.13)(45) \\ &= 5.85 \text{ in.} \end{aligned} \quad (\text{B.22})^*$$

By solving for  $r_c$  from equations (B.17)

$$\begin{aligned} r_c &= \frac{1}{2} \left( \frac{113}{154.8} + 0.73 \right) \\ &= 0.73 \text{ in.} \end{aligned} \quad (\text{B.23})^*$$

According to equation (5.25)

$$L_c \geq 4r_c$$

or

$$\frac{L_c}{r_c} \geq 4,$$

as a check

$$\frac{5.85}{0.73} = 8.01$$

therefore the condition is satisfied. Using equation (B.16) to solve for  $r_w$  gives

$$r_w = \frac{1}{2} \left[ \frac{113}{154.8} + 26.93 + 2(5.85) \right]$$

$$= 19.70 \text{ in.}$$

(B.24)\*

XII. APPENDIX C: HEAT TRANSFER CALCULATIONS FOR  
PROTOTYPE NITINOL TUBE

This appendix undertakes four tasks. The first is to calculate the value of the heat transfer coefficient for convection. The second task is to determine the pressure drop experienced by the water as it passes through the tube. Next, the time required for the tube to undergo transformation upon the introduction of water at high temperature is found. Finally, an approximation is made of the amount of heat delivered to the tube during a cycle.

The principal assumptions made in this appendix are: (1) The Nitinol's composition is such that its transformation temperature is  $65^{\circ}\text{F}$ , (2) The inside diameter of the Nitinol tube is 0.25 inches, and (3) The flow rate of the water passing through the tube is one gallon per minute. The first two assumptions are based on experimental data contained in Cross et al. (13), and the choice of flow rate was made arbitrarily although it is felt that the value chosen is reasonable.

As given in Appendix B, equation (B.11)

$$A_T^C = 2.0 \times 10^{-2} \text{ in}^2$$

but  $A_T^C$  is related to the tube's inside and outside diameters by

$$A_T^C = \frac{\pi}{4} [D_o^2 - D_i^2]$$

from assumption (2),

$$D_i = 0.25 \text{ in.}, \quad (\text{C.1})$$

therefore

$$\begin{aligned}
 D_0 &= \left\{ D_i^2 + \frac{4}{\pi} A_T^c \right\}^{1/2} \\
 &= \left\{ (0.25 \text{ in})^2 + \frac{4}{\pi} (2.0 \times 10^{-2} \text{ in}^2) \right\}^{1/2} \\
 &= 0.30 \text{ in.}
 \end{aligned}$$

The thickness of the tube is then

$$\begin{aligned}
 \Delta r &= \frac{1}{2} (D_0 - D_i) \\
 &= \frac{1}{2} (0.30 - 0.25) \\
 &= 2.5 \times 10^{-2} \text{ in.} \tag{C.2}
 \end{aligned}$$

The value of the water flowrate, as given in the third assumption, is used to determine the Reynold's number by the formula

$$\text{Re} = \frac{\rho_w U_w D_i}{\mu_w}, \tag{C.3}$$

where the density of the water  $\rho_w$  is  $62.4 \text{ lbm/ft}^3$ , and the water's viscosity  $\mu_w$ , at  $115^\circ\text{F}$ , is  $1.42 \frac{\text{lbm}}{\text{ft hr}}$  (31). Converting the water flow rate  $\dot{V}$  into the corresponding water velocity

$$U_w = \frac{\dot{V}}{A_T^c}$$

gives



$$\begin{aligned}
 U_w &= \frac{(1\text{gpm})(144 \text{ in}^2/\text{ft}^2)(60 \frac{\text{min}}{\text{hr}})}{(2.0 \times 10^{-2} \text{ in}^2)(7.48 \text{ gal}/\text{ft}^3)} \\
 &= 5.8 \times 10^4 \frac{\text{ft}}{\text{hr}}.
 \end{aligned}
 \tag{C.4}$$

Substituting this and equation (C.1) into equation (C.3) results in a Reynold's number  $Re$  of

$$\begin{aligned}
 Re &= \frac{(62.4 \frac{\text{lbm}}{\text{ft}^3})(5.8 \times 10^4 \frac{\text{ft}}{\text{hr}})(0.25 \text{ in})}{(12 \text{ in}/\text{ft})(1.42 \frac{\text{lbm}}{\text{ft hr}})} \\
 &= 5.3 \times 10^4
 \end{aligned}
 \tag{C.5}$$

According to Perry and Chilton (32) the following correlation holds for  $Re > 10^4$  and  $10 < L/D < 400$

$$\frac{h_i D_i}{k_w} = 0.036 Re^{0.8} \left( \frac{C_{p_w} \mu_w}{k_w} \right)^{1/3} \left( \frac{L}{D_i} \right)^{-0.054}
 \tag{C.6}$$

where, for this prototype

$$\begin{aligned}
 \frac{L}{D_i} &= \frac{9.10 \text{ in}}{0.25 \text{ in}} \\
 &= 36.4.
 \end{aligned}
 \tag{C.7}$$

For a water temperature of  $115^\circ\text{F}$  the values for the thermal conductivity of water  $k_w$  and the specific heat  $C_{p_w}$  are (31)  $0.368 \frac{\text{Btu}}{\text{hr ft } ^\circ\text{F}}$  and  $1.0 \frac{\text{Btu}}{\text{lbm } ^\circ\text{F}}$ , respectively. Then from equation (C.6) the heat transfer

coefficient for convection is

$$\begin{aligned}
 h_i &= \frac{(0.368 \frac{\text{Btu}}{\text{hr ft } ^\circ\text{F}})(12 \text{ in/ft})}{(0.25 \text{ in})} 0.036 (5.3 \times 10^4)^{0.8} \\
 &\times \left[ \frac{(1 \frac{\text{Btu}}{\text{lbm } ^\circ\text{F}})(1.42 \frac{\text{lbm}}{\text{ft hr}})}{0.368 \frac{\text{Btu}}{\text{hr ft } ^\circ\text{F}}} \right]^{1/3} (36.4)^{-0.054} \\
 &= 4943 \frac{\text{Btu}}{\text{hr ft}^2 ^\circ\text{F}} \tag{C.8}
 \end{aligned}$$

For a given Reynolds number the following equation can be used to determine the pressure drop experienced by water flowing through a tube (31)

$$\frac{\Delta U_w^2}{2g_c} + \frac{g}{g_c} \Delta Z + \frac{\Delta P}{\rho_w} + l w_f = 0 \tag{C.9}$$

where  $g_c$  is a conversion constant

$$g_c = 32.17 \frac{\text{lbm ft}}{\text{lbf sec}^2},$$

$g$  is the local acceleration of gravity and is usually given the value

$$g = 32.2 \frac{\text{ft}}{\text{sec}^2},$$

$\Delta Z$  is the vertical change in position which in this case will be equivalent to the tube length

$$\Delta Z = L_T = 9.83 \text{ in.}$$

$$= 0.82 \text{ ft.},$$

and  $lw_f$  is the lost work due to pipe friction, where (31)

$$lw_f = \frac{2f l_e U^2}{g_c D_i} \quad (C.10)$$

The friction factor  $f$  in equation (C.10) is approximately equal to 0.005 (32) for smooth pipe (e.g. drawn tube) and for the value of  $Re$  given in equation (C.5). The term  $l_e$  in equation (C.10) is the equivalent length of the tube which includes the effects of the two  $90^\circ$  square bends (figure 6). The equivalent length of one square bend, in 0.25 inch tube, is approximately (31) 1.3 ft., thus the equivalent length of the tube is

$$\begin{aligned} l_e &= 0.82 \text{ ft} + 2 (1.3 \text{ ft}) \\ &= 3.42 \text{ ft.} \end{aligned}$$

Substituting this and the value given for  $f$  into equation (C.10) yields

$$\begin{aligned} lw_f &= \frac{2(0.005)(3.42 \text{ ft})(5.8 \times 10^4 \frac{\text{ft}}{\text{hr}})^2 (12 \text{ in/ft})}{(32.17 \frac{\text{lbm ft}}{\text{lbf sec}^2})(0.25 \text{ in})(3600 \frac{\text{sec}}{\text{hr}})^2} \\ &= 13.2 \frac{\text{ft lbf}}{\text{lbm}} \end{aligned}$$

Solving equation (C.9) for  $\Delta P$  gives

$$\begin{aligned}
\Delta P &= \rho_w \left[ -\frac{\Delta U_w^2}{2g_c} - \frac{g}{g_c} \Delta Z - lw_f \right] = (62.4 \text{ lbm/ft}^3) \\
&\times \left[ -\frac{\{(5.8 \times 10^4 \frac{\text{ft}}{\text{hr}}) - (5.8 \times 10^4 \frac{\text{ft}}{\text{hr}})\}^2}{2(32.17 \frac{\text{lbm ft}}{\text{lbf sec}^2})} - \frac{32.2 \frac{\text{ft}}{\text{sec}^2}}{32.17 \frac{\text{lbm ft}}{\text{lbf sec}^2}} (0.82 \text{ ft}) \right. \\
&\quad \left. - 13.2 \frac{\text{ft lbf}}{\text{lbm}} \right] \\
&= -874.9 \frac{\text{lbf}}{\text{ft}^2} \\
&= -6.1 \text{ psi} \tag{C.11}
\end{aligned}$$

as the pressure drop for the water flowing through one tube.

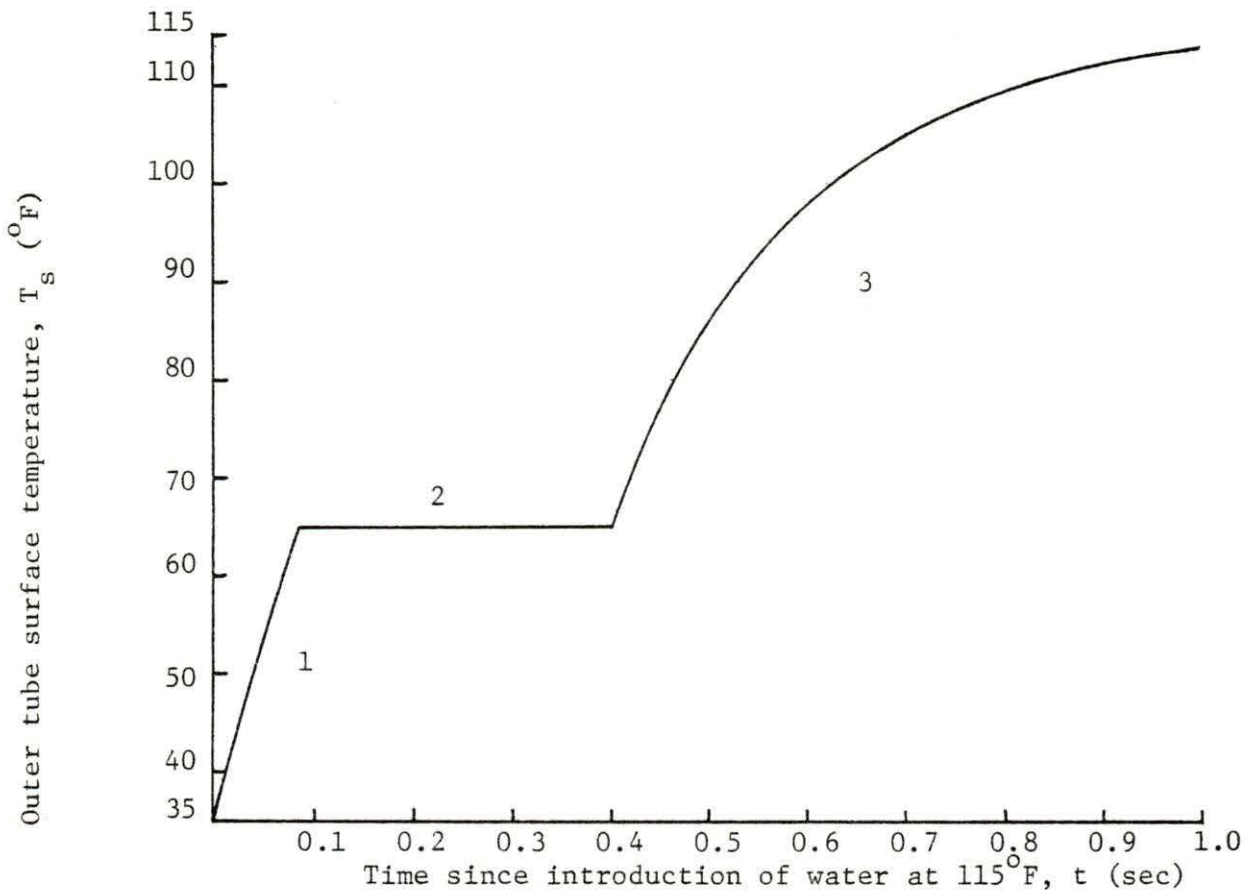
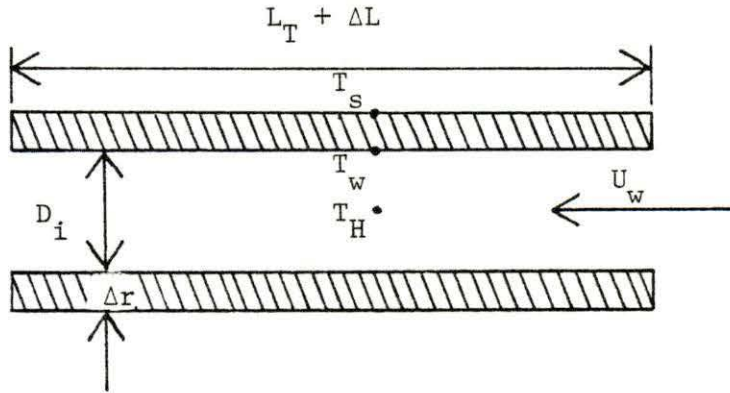
Figure 11(a) is a representation of a Nitinol tube with water at 115°F flowing through it. The rate at which heat is transferred through the internal thermal boundary layer to the tube can be expressed as

$$h_i A_i (T_H - T_w) = M_T C_{p_N} \frac{dT}{dt} \tag{C.12}$$

where the internal tube surface area  $A_i$  is

$$\begin{aligned}
A_i &= \pi D_i (L_T + \Delta L) \\
&= (0.25 \text{ in})(9.83 \text{ in}) / 144 \text{ in}^2/\text{ft}^2 \\
&= 5.4 \times 10^{-2} \text{ ft}^2
\end{aligned}$$

and  $C_{p_t}$  is given as (3)



(b)

Figure 11. Temperature relationships with position and time (a) Model of temperature distribution in Nitinol tube element; (b) Plot of outer tube surface temperature  $T_s$  versus time for Nitinol tube

$$C_{pN} = \begin{cases} 0.150 \frac{\text{Btu}}{\text{lbm } ^\circ\text{F}}, & 35^\circ\text{F} < T_s < 65^\circ\text{F} \\ 0.153 \frac{\text{Btu}}{\text{lbm } ^\circ\text{F}}, & 65^\circ\text{F} < T_s < 115^\circ\text{F}. \end{cases} \quad (\text{C.13})$$

At the same time the rate of heat transfer through the tube wall is

$$k_N \frac{A_{1m}}{\Delta r} (T_w - T_s) = M_T C_{pN} \frac{dT}{dt} \quad (\text{C.14})$$

in which  $k_N$  is the coefficient of thermal conductivity and has the value (3)

$$k_N = 9.54 \frac{\text{Btu}}{\text{hr ft } ^\circ\text{F}},$$

and  $A_{1m}$  is the log mean surface area of the tube where

$$\begin{aligned} A_{1m} &= \frac{A_o - A_i}{\ln \left( \frac{A_o}{A_i} \right)} \\ &= \frac{\pi (D_o - D_i) L}{\ln \left( \frac{D_o}{D_i} \right)} \\ &= \frac{\pi (0.30 \text{ in.} - 0.25 \text{ in.}) (9.83 \text{ in.})}{(144 \frac{\text{in}^2}{\text{ft}^2}) \ln \left( \frac{0.30}{0.25} \right)} \\ &= 5.9 \times 10^{-2} \text{ ft}^2. \end{aligned}$$

From equation (C.12)

$$T_w = T_H - \frac{M_T C_{PN}}{h_i A_i} \frac{dT}{dt} \quad (C.15)$$

Substituting equation (C.15) into equation (C.14) gives

$$k \frac{A_{lm}}{\Delta r} (T_H - \frac{M_T C_{PN}}{h_i A_i} \frac{dT}{dt} - T_s) = M_T C_{PN} \frac{dT}{dt}$$

$$T_H - T_s = M_T C_{PN} \left( \frac{\Delta r}{k A_{lm}} + \frac{1}{h_i A_i} \right) \frac{dT}{dt}$$

$$dt = M_T C_{PN} \left( \frac{\Delta r}{k A_{lm}} + \frac{1}{h_i A_i} \right) \frac{dT}{(T_H - T_s)}$$

Integrating both sides of the above equation results in

$$\int_{t_o}^t dt = M_T C_{PN} \left( \frac{\Delta r}{k A_{lm}} + \frac{1}{h_i A_i} \right) \int_{T_s=35^\circ F}^{T_s} \frac{dT}{T_H - T_s}$$

$$t = t_o + M_T C_{PN} \left( \frac{\Delta r}{k A_{lm}} + \frac{1}{h_i A_i} \right) \ln \left( \frac{T_H - 35}{T_H - T_s} \right) \quad (C.16)$$

For the case where  $35^\circ F < T_s < 65^\circ F$  and  $T_H = 115^\circ F$ , let  $t_o = 0$  hr, then equation (C.16) gives the temperature distribution of  $T_s$  with respect to time as shown by curve 1 in figure 11(b).

When  $T_s = 65^\circ F$ , it is assumed that the tube transforms to the high temperature phase. However, a certain amount of time is required for the Nitinol to absorb the heat needed to accomplish the transformation reaction. This required heat is the latent heat of transformation,  $\Delta H$ .

The value of  $\Delta H$  is given by Jackson et al. (3) to be 12.3 Btu per pound of Nitinol. Also, as this heat for transformation is being absorbed by the tube material the tube temperature does not change so that  $T_s$  remains constant at the transformation temperature of  $65^\circ\text{F}$ . Thus for the case of transformation

$$h_i A_i (T - T_w) = \frac{M_T d\Delta H}{dt},$$

solving for  $T_w$  gives

$$T_w = T_H - \frac{M_T}{h_i A_i} \frac{d\Delta H}{dt}. \quad (\text{C.17})$$

For heat flow through the tube wall

$$k_N \frac{A_{lm}}{\Delta r} (T_w - T_s) = \frac{M_T \Delta H}{dt}, \quad (\text{C.18})$$

substituting equation (C.17) into equation (C.18) and solving for  $dt$  yields

$$dt = \frac{M_T}{T_H - T_s} \left( \frac{\Delta r}{k_N A_{lm}} + \frac{1}{h_i A_i} \right) d\Delta H. \quad (\text{C.19})$$

Integrating both sides of equation (C.19) results in

$$\int_{t_1}^t dt = \frac{M_T}{T_H - T_s} \left( \frac{\Delta r}{k_N A_{lm}} + \frac{1}{h_i A_i} \right) \int_0^{\Delta H} d\Delta H$$

$$t = t_1 + \frac{M_T}{T_H - T_s} \left( \frac{\Delta r}{k_N A_{lm}} + \frac{1}{h_i A_i} \right) \Delta H \quad (\text{C.20})$$



where for this case  $t_1$  is given by equation (C.16) when  $T_s = 65^\circ\text{F}$ . The temperature-time relationship expressed by equation (C.20) is illustrated by curve 2 in figure 11(b).

By methods similar to those used to derive equation (C.16) the expression for curve 3 in figure 11(b), is

$$t = t_2 + M_T C_{P_N} \left( \frac{\Delta r}{kA_{lm}} + \frac{1}{h_i A_i} \right) \ln \left( \frac{T_H - 65}{T_H - T_s} \right) \quad (\text{C.21})$$

where  $C_{P_N}$  is given by equation (C.13) and  $t_2$  is given by equation (C.20).

As shown in figure 11(b),  $T_s$  reaches a value of about 95% of  $T_H$  at  $t = 1$  second, this then is the time for the heating half of the cycle. The amount of heat delivered to the tube during heating can be approximated from equation (C.12) for curves 1 and 3, and for curve 2 from equation (C.18) thus

$$\begin{aligned} Q_1 &\approx M_T C_{P_N} \Delta T \\ &= (4.6 \times 10^{-2} \text{ lb}_m) \left( 0.150 \frac{\text{Btu}}{\text{lb}_m \text{ } ^\circ\text{F}} \right) (65^\circ\text{F} - 35^\circ\text{F}) \\ &= 0.21 \text{ Btu} \end{aligned}$$

$$\begin{aligned} Q_2 &\approx M_T \Delta H \\ &= (4.6 \times 10^{-2} \text{ lb}_m) \left( 12.3 \frac{\text{Btu}}{\text{lb}_m} \right) \end{aligned}$$

$$\begin{aligned}Q_3 &\approx M_T C_{P_N} \Delta T \\&= (4.6 \times 10^{-2} \text{ lbm}) \left( 0.153 \frac{\text{Btu}}{\text{lbm}^\circ\text{F}} \right) (115^\circ\text{F} - 65^\circ\text{F}) \\&= 0.35 \text{ Btu}\end{aligned}$$

therefore

$$\begin{aligned}Q &= Q_1 + Q_2 + Q_3 \\&= 0.21 \text{ Btu} + 0.56 \text{ Btu} + 0.35 \text{ Btu} \\&= 1.12 \text{ Btu}\end{aligned}$$

$$= 1.75 \text{ bar}$$

$$= 0.578 \text{ bar} + 0.000000 + 0.000000$$

$$0 = 0^1 + 0^3 + 0^3$$

$$= 0.75 \text{ bar}$$

$$= (0.75 \text{ bar}) \left( \frac{1.0}{1.0} \right) \left( \frac{1.0}{1.0} \right) \left( \frac{1.0}{1.0} \right)$$

$$0^3 = 0^3 + 0^3 + 0^3$$